Exploiting Multi-Antennas for Opportunistic Spectrum Sharing in Cognitive Radio Networks

Rui Zhang, *Member, IEEE,* Ying-Chang Liang, *Senior Member, IEEE*

Abstract

In cognitive radio (CR) networks, there are scenarios where the secondary (lower priority) users intend to communicate with each other by opportunistically utilizing the transmit spectrum originally allocated to the existing primary (higher priority) users. For such a scenario, a secondary user usually has to trade off between two conflicting goals at the same time: one is to maximize its own transmit throughput; and the other is to minimize the amount of interference it produces at each primary receiver.

In this paper, we study this fundamental tradeoff from an information-theoretic perspective by characterizing the secondary user's channel capacity under both its own transmit-power constraint as well as a set of interference-power constraints each imposed at one of the primary receivers. In particular, this paper exploits multi-antennas at the secondary transmitter to effectively balance between spatial multiplexing for the secondary transmission and interference avoidance at the primary receivers. Convex optimization techniques are used to design algorithms for the optimal secondary transmit spatial spectrum that achieves the capacity of the secondary transmission. Suboptimal solutions for ease of implementation are also presented and their performances are compared with the optimal solution. Furthermore, algorithms developed for the single-channel transmission are also extended to the case of multi-channel transmission whereby the secondary user is able to achieve opportunistic spectrum sharing via transmit adaptations not only in space, but in time and frequency domains as well. Simulation results show that even under stringent interference-power constraints, substantial capacity gains are achievable for the secondary transmission by employing multi-antennas at the secondary transmitter. This is true even when the number of primary receivers exceeds that of secondary transmit antennas in a CR network, where an interesting "interference diversity" effect can be exploited.

Index Terms

Cognitive radio (CR), opportunistic spectrum sharing, multiple-input multiple-output (MIMO), channel capacity, dynamic resource allocation, interference diversity, convex optimization.

Manuscript received on May 18, 2007; revised on August 29, 2007. This paper was presented in part at IEEE International Symposium on Personal, Indoor and Mobile Radio Communications (PIMRC), Athens, Greece, September 2007.

The authors are with the Institute for Infocomm Research, 21 Heng Mui Keng Terrace, 119613 Singapore (e-mails:{rzhang, ycliang}@i2r.a-star.edu.sg).

I. Introduction

Fixed spectrum allocation is the major spectrum allocation methodology for traditional wireless communication services. In particular, in order to avoid interference, different wireless services are allocated with different licensed bands. With the popularity of various wireless technologies, fixed spectrum allocation strategy has resulted in scarcity in radio spectrum, due to the fact that most of the available spectrum has been allocated. Because of the spectrum scarcity, one immediate consequence is that, while there are a lot of research activities dealing with technical issues related to the fourth-generation (4G) cellular systems, it is still unclear which frequency band is available for such systems. On the other hand, recent measurements by FCC and others have shown that more than 70% of the allocated spectrum in United States is not utilized [1]. Furthermore, the spectrum utilization varies in space, time and frequency. This motivates the invention of cognitive radio (CR) network [2]-[3], which supports *opportunistic spectrum sharing* by allowing the secondary (lower priority) users to share the radio spectrum originally allocated to the primary (higher priority) users. By doing so, the utilization efficiency of the radio spectrum can be significantly enhanced.

In CR networks, the primary users have a higher priority than the secondary users in utilizing spectrum resource, therefore, one fundamental challenge by introducing opportunistic spectrum sharing is to ensure the quality-of-service (QoS) of the primary users while maximizing the achievable throughput of the secondary users. Recently, there has been a great deal of research related to this interesting problem. When the primary users are legacy systems that do not actively participate in transmit power control, the QoS of the primary users is maintained by introducing interference-power constraint measured at the primary receiver. That is to say, the interference power received at the primary receiver should be less than a threshold. Under this setup, a seminal work in [4] studied the channel capacity of a single secondary transmission under a set of receiver-side power constraints instead of the conventional transmitter-side power constraints. In [5], the ergodic capacity of the secondary transmission link in a fading environment is studied under instantaneous or average interference-power constraint at a single primary receiver. When multiple secondary users share a single-frequency channel advertised by the primary user, the authors in [6]-[7] utilize the game theory to maximize the sum of the utility functions of the secondary users under the interference-power constraint at some measured point, while in [8]-[9] transmit resource allocation for the secondary users is studied by applying the graph-theoretic models. Recent information-theoretic studies on CR networks can also be found in, e.g., [10]-[15].

Most prior research on radio resource allocation for CR networks focuses on time and/or frequency domains, while assuming single antenna employed at both primary and secondary transceivers. Wireless transmissions via multiple transmit antennas and multiple receive antennas, or the so-called multiple-input multiple-output (MIMO) transmissions, have received considerable attention during the past decade. Multi-antennas can be utilized to achieve many desirable functions for wireless transmissions, such as folded capacity increase without bandwidth expansion (e.g., [16]-[18]), dramatic enhancement of transmission reliability via space-time coding (e.g., [19]-[20]), and effective co-channel interference suppression for multiuser transmissions (e.g., [21]). However, the role of multi-antennas in a CR network is yet completely understood. Generally speaking, multi-antennas can be used to allocate transmit dimensions in space and hence provide the secondary transmitter in a CR network more degrees of freedom in space in addition to time and frequency so as to balance between maximizing its own transmit rate and minimizing the interference powers at the primary receivers. This motivates the research of this paper to be done, with an aim to address fundamentally the MIMO channel capacity of a secondary user under optimum spectrum sharing in a CR network.

The main contributions of this paper are summarized as follows:

- This paper formulates the design of capacity-achieving transmit spatial spectrum for a single secondary link in a CR network under both its own transmit-power constraint and a set of interference-power constraints at the primary receivers as a sequence of *convex* optimization problems. Thanks to convexity of these formulated problems, efficient numerical algorithms are proposed to obtain the optimal secondary transmit spatial spectrum for any arbitrary number of secondary transmit and receive antennas, as well as primary receivers each having single or multiple antennas.
- In the case where the secondary user's channel is multiple-input single-output (MISO), i.e., there is only a single antenna at the secondary receiver, this paper proves that *beamforming* is the optimal strategy for the secondary transmission. For the special case where there is only one single-antenna primary receiver, we are able to derive the closed-form solution for the optimal beamforming vector at the secondary transmitter. For the more general MIMO case where multiple antennas are equipped at both the secondary transmitter and receiver, this paper presents two suboptimal algorithms to tradeoff between *spatial multiplexing* for the secondary transmission and interference avoidance at the primary receivers. One algorithm is based on the singular-value decomposition (SVD) of the secondary user's MIMO channel directly and is thus referred

to as the *Direct-Channel SVD* (D-SVD); and the other is based on the SVD of the secondary MIMO channel after the projection into the null space of the channel from the secondary transmitter to the primary receivers (thereby removing completely the interference at all primary receivers) and is thus referred to as the *Projected-Channel SVD* (P-SVD).

- In the case of multiple primary receivers with single or multiple antennas, a *hybrid* D-SVD/P-SVD algorithm is proposed to remove partially, as opposed to completely in the case of P-SVD, the interferences at the primary receivers. An interesting and novel *interference diversity* effect is discovered and exploited.
- At last, this paper extends the developed algorithms for the single-channel transmission to the case of multi-channel transmission whereby the secondary transmitter is able to adapt transmit resources like transmit spatial spectrum, power and rate in both space and time/freqeuncy for opportunistic spectrum sharing. This paper shows that the multi-channel resource allocation problem can be efficiently solved using the *Lagrange dual-decomposition method* that decomposes the original problem into a set of smaller-size subproblems each for one of the sub-channels.

In [4], Gastpar also considered the MIMO channel capacity for the spectrum sharing scenario. Since only the interference-power constraint is considered in [4], it requires that there exist multiple primary receivers/antennas such that the channel matrix from the secondary transmitter to the primary receivers/antennas is invertible, and by doing so, an upper-bound of the secondary user's MIMO channel capacity is derived by transforming the set of receiver-side power constraints into a transmitter-side power constraint. In contrast, in this paper we consider the MIMO channel capacity for the secondary user under both the interference-power constraints at the primary receivers as well as an explicit transmit-power constraint for the secondary user. With addition of this explicit transmitter-side power constraint, we are able to quantify the exact channel capacity for the secondary user for any arbitrary number of primary receivers/antennas.

This paper is organized as follows. Section II provides the system model of a CR network under opportunistic spectrum sharing, and presents the general problem formulation for transmit optimization of the secondary user. Section III presents the solution for the simplest case where there is only one single-antenna primary receiver, and both primary and secondary users share the same single-channel for transmission. Section IV and Section V extend the solutions to incorporate multiple primary receivers/antennas and the multi-channel transmission, respectively. Section VI provides the simulation results. Finally, Section VII concludes the paper.

The following notations are used in this paper. $|\boldsymbol{S}|$ denotes the determinant, and $\texttt{Tr}(\boldsymbol{S})$ the trace of a square matrix $\boldsymbol{S}$, and $\boldsymbol{S} \succeq 0$ means that $\boldsymbol{S}$ is a positive semi-definite matrix. For any general matrix $\boldsymbol{M}$, $\boldsymbol{M}^{\dagger}$ denotes its conjugate transpose, and $\texttt{Rank}(\boldsymbol{M})$ denotes its rank. $\boldsymbol{I}$ denotes the identity matrix. $\mathbb{E}[\cdot]$ denotes statistical expectation. $\mathbb{C}^{x \times y}$ denotes the space of $x \times y$ matrices with complex entries. The distribution of a circularly-symmetric-complex-Gaussian (CSCG) vector with the mean vector $\boldsymbol{x}$ and the covariance matrix $\boldsymbol{\Sigma}$ is denoted by $\mathcal{CN}(\boldsymbol{x}, \boldsymbol{\Sigma})$, and $\sim$ means "distributed as". The quantity $\min(x, y)$ and $\max(x, y)$ denote, respectively, the minimum and the maximum between two real numbers, x and y, and $(x)^{+} \triangleq \max(x, 0)$. The quantity $||\boldsymbol{x}||$ denotes the Euclidean norm of a vector (also for a scalar) $\boldsymbol{x}$, i.e., $||\boldsymbol{x}||^2 = \texttt{Tr}(\boldsymbol{x}\boldsymbol{x}^{\dagger})$. $\texttt{Re}(x)$ and $\texttt{Im}(x)$ denote the real and imaginary part of a complex number x, respectively.

II. System Model and Problem Formulation

This paper considers a CR network with K primary receivers and a single pair of secondary transmitter and receiver as shown in Fig. 1. It is assumed that all the primary users and the secondary user share the same bandwidth for transmission. This paper considers the scenario where multiple antennas are equipped at the secondary transmitter and possibly at the secondary receiver and each of the primary receivers. It is assumed that the MIMO/MISO channels from the secondary transmitter to the secondary and primary receivers are perfectly known at the secondary transmitter. Under such assumptions, the secondary transmitter is able to adapt its transmit resources such as transmit rate, power, and spatial spectrum based upon the channel knowledge so as to optimally balance between maximizing its own transmit throughput and avoiding interferences at the primary receivers. In practice, the channel from the secondary transmitter to the primary receiver can be obtained at the secondary transmitter by, e.g., periodically sensing the transmitted signal from the primary receiver provided that time-division-duplex (TDD) is employed by the primary transmission. In a fading environment, there are cases where it is difficult for the secondary transmitter to perfectly estimate instantaneous channels. In such cases, the results obtained in this paper provide capacity upper-bounds for the secondary transmission in a CR network.

Consider first a single-channel transmission (e.g., narrow-band transmission with deterministic channels) for both primary and secondary users. The extension to the multi-channel transmission (e.g., multi-tone transmission in frequency or consecutive block-fading channels in time) is considered later in Section V of this paper. In the single-channel case, the secondary transmission can be represented by

$$\boldsymbol{y}(n) = \boldsymbol{H}\boldsymbol{x}(n) + \boldsymbol{z}(n). \tag{1}$$

In the above, $\boldsymbol{H} \in \mathbb{C}^{M_{r,s} \times M_{t,s}}$ denotes the secondary user's channel (assumed to be full rank) where $M_{r,s}$ and $M_{t,s}$ are the number of antennas at the secondary receiver and transmitter, respectively; $\boldsymbol{y}(n)$ and $\boldsymbol{x}(n)$ are the received and transmitted signal vector, respectively, and n is the symbol index; $\boldsymbol{z}(n)$ is the additive noise vector at the secondary receiver, and it is assumed that $\boldsymbol{z}(n) \sim \mathcal{CN}(0, \boldsymbol{I})$.[1] Let the transmit covariance matrix (or spatial spectrum) of the secondary user be denoted by $\boldsymbol{S}$, $\boldsymbol{S} = \mathbb{E}[\boldsymbol{x}(n)\boldsymbol{x}^{\dagger}(n)]$, where the expectation is taken over the code-book. Since this paper characterizes the information-theoretic limit of the secondary transmission, it is assumed that the ideal Gaussian code-book with infinitely large number of codeword symbols is used, i.e., $\boldsymbol{x}(n) \sim \mathcal{CN}(0, \boldsymbol{S}), n = 1, 2, \ldots, \infty$. The transmit covariance matrix $\boldsymbol{S}$ can be further represented by its eigenvalue decomposition expressed as

$$\boldsymbol{S} = \boldsymbol{V}\boldsymbol{\Sigma}\boldsymbol{V}^{\dagger}, \tag{2}$$

where $\boldsymbol{V} \in \mathbb{C}^{M_{t,s} \times d}$, $\boldsymbol{V}^{\dagger}\boldsymbol{V} = \boldsymbol{I}$, contains the eigenvectors of $\boldsymbol{S}$, and is also termed in practice as the *precoding matrix* because each column of $\boldsymbol{V}$ is the precoding vector for one transmitted data stream; d, $d \leq M_{t,s}$, is usually referred to as the degree of *spatial multiplexing* because it measures the number of transmit dimensions (or equivalently, the number of data streams) in the spatial domain; $\boldsymbol{\Sigma}$ is a $d \times d$ diagonal matrix, and its diagonal elements, denoted by $\sigma_1, \sigma_2, \ldots, \sigma_d$, are the positive eigenvalues of $\boldsymbol{S}$, and also represent the assigned transmit powers for their corresponding data streams. Notice that $\texttt{Rank}(\boldsymbol{S}) = d$. If $d = 1$, the corresponding transmission strategy is usually termed as *beamforming* while in the case of $d > 1$, it is termed as *spatial multiplexing*. The transmit power P for each block is limited by the secondary user's own transmit power constraint denoted by P_t, i.e., it holds that $P = \texttt{Tr}(\boldsymbol{S}) = \sum_{i=1}^{d} \sigma_i \leq P_t$.

Assuming that there are K primary receivers in the CR network, each equipped with M_k receive antennas, $k = 1, \ldots, K$. For each primary receiver, there may be a total interference-power constraint over all receive antennas or a set of interference-power constraints applied to each individual receive antenna. The former case can be expressed as

$$\sum_{j=1}^{M_k} \boldsymbol{g}_{k,j}\boldsymbol{S}\boldsymbol{g}_{k,j}^{\dagger} \leq \Gamma_k, \quad k = 1, \ldots, K, \tag{3}$$

where $\boldsymbol{g}_{k,j} \in \mathbb{C}^{1 \times M_{t,s}}$ represents the channel from the secondary transmitter to the j-th receive antenna of the k-th primary receiver, and Γ_k is the total interference-power constraint over all receive antennas for the k-th primary

[1] The noise at the secondary receiver may also contain the interference from the primary transmitters (not shown in Fig. 1) and is thus non-white in general. However, by applying a noise-whitening filter at the secondary receiver and incorporating this filter matrix into the channel matrix $\boldsymbol{H}$, the equivalent noise at the secondary receiver can be assumed to be approximately white Gaussian.

receiver. Let $\boldsymbol{G}_k \in \mathbb{C}^{M_k \times M_{t,s}}$ (assumed to be full-rank) be the equivalent channel matrix from the secondary transmitter to the k-th primary receiver obtained by stacking all $\boldsymbol{g}_{k,j}$, $j = 1, \ldots, M_k$, into $\boldsymbol{G}_k$. Using $\boldsymbol{G}_k$'s, (3) can be thus rewritten as

$$\mathtt{Tr}\left(\boldsymbol{G}_k \boldsymbol{S} \boldsymbol{G}_k^{\dagger}\right) \leq \Gamma_k, \quad k = 1, \ldots, K. \tag{4}$$

The latter case can be represented as

$$\boldsymbol{g}_{k,j} \boldsymbol{S} \boldsymbol{g}_{k,j}^{\dagger} \leq \gamma_k, \quad j = 1, \ldots, M_k, k = 1, \ldots, K, \tag{5}$$

where γ_k is the interference-power constraint applied to each antenna of the k-th primary receiver, and is assumed to be identical for all of its receive antennas. Notice that if $\Gamma_k = M_k \gamma_k$, the per-antenna power constraint in (5) is more stringent than the total-power constraint in (3). On the other hand, (5) can be considered as a special case of (3) because if each receive antenna is treated as an independent primary receiver, (5) is equivalent to (3) if a total number of $M_{r,p} = \sum_{k=1}^{K} M_k$ single-antenna primary receivers are assumed. Therefore, for the rest of this paper, the total interference-power constraint in (3) or (4) is considered as the generalized interference-power constraint at each primary receiver.

The use of total interference-power constraint at each primary receiver can be further justified by the following theorem:

Theorem 1: The capacity loss of the k-th primary transmission, $k = 1, 2, \ldots, K$, due to the interference from the secondary transmitter with transmit covariance matrix $\boldsymbol{S}$ that satisfies the set of total interference-power constraints in (4) is upper-bounded by $\min(M_k, N_k) \log_2\left(1 + \frac{\Gamma_k}{\phi_k}\right)$ bits/complex dimension, where N_k and M_k are the number of transmit and receiver antennas for the k-th primary user, respectively, and ϕ_k is the additive white Gaussian noise power at its receiver.

Proof: Please refer to Appendix I. ■

From Theorem 1, it follows that by imposing the total interference-power constraint, it is ensured that the capacity loss of each primary user due to the secondary transmission is well regulated. Notice that the obtained upper-bound for the capacity loss is not a function of the primary/secondary user's channels, or their transmit covariance matrices. By choosing Γ_k to be sufficiently small compared with the noise power at each primary receiver, e.g., $\Gamma_k \ll \phi_k$, the capacity loss due to the secondary transmission can be made arbitrarily small.

At last, we formulate the main problem to be addressed in this paper. We are interested in the design of the spatial spectrum $\boldsymbol{S}$ at the secondary transmitter so as to maximize its transmit rate under both its own transmit-power constraint and a set of total interference-power constraints at K primary receivers. Accordingly, the optimal $\boldsymbol{S}$ can be obtained by solving the following problem (**P1**):

$$\begin{aligned} \texttt{Maximize} \quad & \log_2 \left| \boldsymbol{I} + \boldsymbol{H}\boldsymbol{S}\boldsymbol{H}^\dagger \right| && (6) \\ \texttt{Subject to} \quad & \texttt{Tr}(\boldsymbol{S}) \leq P_t, && (7) \\ & \texttt{Tr}\left(\boldsymbol{G}_k \boldsymbol{S} \boldsymbol{G}_k^\dagger\right) \leq \Gamma_k, \;\; k = 1, \ldots, K && (8) \\ & \boldsymbol{S} \succeq 0. && (9) \end{aligned}$$

The above problem maximizes the secondary user's channel capacity (in bits/complex dimension) obtained by computing the mutual information [22] between the channel input and output in (1), assuming that the secondary user's channel is also known perfectly at the secondary receiver. The constraints in (7) and (8) correspond to the secondary transmitter power constraint and the interference-power constraints at the primary receivers, respectively. (9) is due to the fact that the spectrum matrix $\boldsymbol{S}$ must be positive semi-definite. The problem at hand is a convex optimization problem [23] because its objective function is a concave function of $\boldsymbol{S}$ and all of its constraints specify a convex set of $\boldsymbol{S}$. Therefore, for any arbitrary number of secondary transmit and receive antennas, and primary receivers each having single or multiple antennas, this problem can be efficiently solved by using standard convex optimization techniques, e.g., the interior-point method [23], for which the details are omitted here for brevity. In the sequel, we will investigate further into this problem so as to provide more insightful solutions for it that may not be obtainable from solely a numerical optimization perspective. We will first consider the simplest case where there is only one single-antenna primary receiver at present in Section III, and then consider the general case of multiple primary receivers/antennas in Section IV.

III. One Single-Antenna Primary Receiver

The scenario where there is only one single-antenna primary receiver is considered in this section. Consequently, the channel from the secondary transmitter to the primary receiver is MISO, and can be represented by a vector $\boldsymbol{g} \in \mathbb{C}^{1 \times M_{t,s}}$. Let γ denote the maximum interference power tolerable at the primary receiver. Problem **P1** can be then simplified as (**P2**)

$$\texttt{Maximize} \quad \log_2 \left| \boldsymbol{I} + \boldsymbol{H}\boldsymbol{S}\boldsymbol{H}^\dagger \right| \tag{10}$$

$$\texttt{Subject to} \quad \texttt{Tr}(\boldsymbol{S}) \le P_t, \tag{11}$$

$$\boldsymbol{g}\boldsymbol{S}\boldsymbol{g}^\dagger \le \gamma, \tag{12}$$

$$\boldsymbol{S} \succeq 0. \tag{13}$$

A. MISO Secondary User's Channel

Consider first the case where there is only a single antenna at the secondary receiver, i.e., $M_{r,s} = 1$ and the secondary user's channel is also MISO. Hence, $\boldsymbol{H}$ is in fact a vector and for convenience is denoted by $\boldsymbol{H} \equiv \boldsymbol{h}$, $\boldsymbol{h} \in \mathbb{C}^{1\times M_{t,s}}$. In this case, we are able to derive the closed-form solution for the optimal $\boldsymbol{S}$. First, the following two lemmas are needed:

Lemma 1: In the case of MISO secondary user's channel, the optimal $\boldsymbol{S}$ for Problem **P2** satisfies $\texttt{Rank}(\boldsymbol{S}) = 1$.

Proof: Please refer to Appendix II. ■

Lemma 1 indicates that in the MISO case, *beamforming* is indeed optimal for the secondary transmitter. Therefore, $\boldsymbol{S}$ can be written in the form of $\boldsymbol{S} = \boldsymbol{v}\boldsymbol{v}^\dagger, \boldsymbol{v} \in \mathbb{C}^{M_{t,s}\times 1}$. Problem **P2** can be then simplified as

$$\texttt{Maximize} \quad \log_2 \left(1 + ||\boldsymbol{h}\boldsymbol{v}||^2\right) \tag{14}$$

$$\texttt{Subject to} \quad ||\boldsymbol{v}||^2 \le P_t, \tag{15}$$

$$||\boldsymbol{g}\boldsymbol{v}||^2 \le \gamma. \tag{16}$$

The second lemma then provides the optimal structure of $\boldsymbol{v}$:

Lemma 2: In the case of MISO secondary user's channel, the optimal beamforming vector $\boldsymbol{v}$ is in the form of $\alpha_v \hat{\boldsymbol{g}} + \beta_v \hat{\boldsymbol{h}}_\perp$, where $\hat{\boldsymbol{g}} = \frac{\boldsymbol{g}^\dagger}{||\boldsymbol{g}||}$ and $\hat{\boldsymbol{h}}_\perp = \frac{\boldsymbol{h}_\perp}{||\boldsymbol{h}_\perp||}$, $\boldsymbol{h}_\perp = \boldsymbol{h}^\dagger - (\hat{\boldsymbol{g}}^\dagger \boldsymbol{h}^\dagger)\hat{\boldsymbol{g}}$, α_v and β_v are complex weights.

Proof: Please refer to Appendix III. ■

Lemma 2 states that the optimal beamforming vector should lie in the space spanned jointly by $\boldsymbol{g}^\dagger$ and the projection of $\boldsymbol{h}^\dagger$ into the null space of $\boldsymbol{g}^\dagger$. Using Lemma 2 and let $\boldsymbol{h}^\dagger = \alpha_h \hat{\boldsymbol{g}} + \beta_h \hat{\boldsymbol{h}}_\perp$, the optimal weights α_v

and β_v can be then obtained by considering the following equivalent problem of that in (14)-(16):

$$\texttt{Maximize} \quad ||\alpha_h^{\dagger}\alpha_v + \beta_h^{\dagger}\beta_v||^2 \tag{17}$$

$$\texttt{Subject to} \quad ||\alpha_v||^2 + ||\beta_v||^2 \leq P_t, \tag{18}$$

$$||\boldsymbol{g}||^2||\alpha_v||^2 \leq \gamma. \tag{19}$$

The above problem can be solved by using standard geometry. Notice that the solution for the above problem is trivial in the case of $\alpha_h = 0$ or $\beta_h = 0$. Hence, without loss of generality, it is assumed that $\alpha_h \neq 0$ and $\beta_h \neq 0$. To summarize, the following theorem is established:

Theorem 2: In the case of MISO secondary user's channel, the optimal transmit covariance matrix $\boldsymbol{S}$ for Problem **P2** can be written in the form of $\boldsymbol{S} = \boldsymbol{v}\boldsymbol{v}^{\dagger}$, where $\boldsymbol{v} = \alpha_v\hat{\boldsymbol{g}} + \beta_v\hat{\boldsymbol{h}}_{\perp}$, and α_v and β_v are given by

- Case I: If $\gamma \geq \frac{||\boldsymbol{g}||^2||\alpha_h||^2}{||\alpha_h||^2+||\beta_h||^2}P_t$,

$$\alpha_v = \sqrt{\frac{P_t}{||\alpha_h||^2 + ||\beta_h||^2}}\alpha_h, \quad \beta_v = \sqrt{\frac{P_t}{||\alpha_h||^2 + ||\beta_h||^2}}\beta_h.$$

- Case II: If $\gamma < \frac{||\boldsymbol{g}||^2||\alpha_h||^2}{||\alpha_h||^2+||\beta_h||^2}P_t$,

$$\alpha_v = \frac{\sqrt{\gamma}}{||\boldsymbol{g}||}\frac{\alpha_h}{||\alpha_h||}, \; \beta_v = \sqrt{P_t - \frac{\gamma}{||\boldsymbol{g}||^2}}\frac{\beta_h}{||\beta_h||}.$$

In Theorem 2, Case I corresponds to the interference-power constraint in (16) being inactive. In this case, it can be verified that $\boldsymbol{v} = \frac{\sqrt{P_t}}{||\boldsymbol{h}||}\boldsymbol{h}^{\dagger}$. Therefore, the optimal beamforming vector is identical to that obtained by the pre-maximal-ratio-combining (MRC) principle for the conventional MISO point-to-point transmission. On the other hand, Case II corresponds to the interference-power constraint being active and, hence, the transmit power $||\alpha_v||^2$ allocated in the direction of $\hat{\boldsymbol{g}}$ needs to be regulated by γ.

B. MIMO Secondary User's Channel

In the case that the secondary user's channel is MIMO, i.e., $M_{t,s} > 1$ and $M_{r,s} > 1$, there is in general no closed-form solution for the optimal $\boldsymbol{S}$, and Problem **P2** needs to be solved numerically. Unlike the MISO case, it is possible that $\texttt{Rank}(\boldsymbol{S}) > 1$ in the MIMO case, which implies that *spatial multiplexing* is optimal instead of beamforming. Without the interference-power constraint in (12), the optimal $\boldsymbol{S}$ for Problem **P2** can be obtained from the SVD of $\boldsymbol{H}$, along with the water-filling (WF) -based power allocation (e.g., [16], [22]). The SVD-based transmission is not only capacity-achieving, but of more practical significance, it diagonalizes the secondary user's MIMO channel matrix and decomposes it into parallel AWGN sub-channels, and thereby, reduces substantially the overall encoding/decoding complexity since independent encoding/decoding can be applied over these sub-channels. Unfortunately, when the interference-power constraint in (12) is applied, the optimal $\boldsymbol{S}$ is in general different from that obtained from the channel SVD, and hence does not diagonalize the secondary user's MIMO channel. As a result, sophisticated encoding and decoding methods need to be used in order to achieve the secondary user's channel capacity. One capacity-achieving method is to use a *single constant-rate* Gaussian code-book [24] to encode the information bits and then spread the coded symbols to all transmit antennas. At the receiver, the maximum-likelihood (ML) -based detection and iterative decoding (e.g., [25]) are applied to decode the whole codeword. Alternatively, the capacity can also be achieved by using *multiple variable-rate* Gaussian code-books each for one of d data streams. At the receiver, these data streams are decoded by optimum decision-feedback-based successive decoding (e.g., [26]-[27]).

This paper presents two suboptimal algorithms that obtain closed-form solutions for $\boldsymbol{S}$ in the case of MIMO secondary user's channel. The computational complexity for both algorithms is much lower than that of the interior-point method for Problem **P2**. Furthermore, both algorithms are based on the SVD of the secondary user's channel matrix and decompose the secondary MIMO channel into parallel sub-channels. The main difference between these two algorithms lies in that, in the first one, the channel decomposition is based on the SVD of $\boldsymbol{H}$ directly and is thus referred to as the *Direct-Channel SVD* (D-SVD), while in the second one, the channel decomposition is based on the SVD of the projection of $\boldsymbol{H}$ into the null space of $\boldsymbol{g}^{\dagger}$, and is thus referred to as the *Projected-Channel SVD* (P-SVD). Notice that these two algorithms can also be applied in the previous case of MISO secondary user's channel to obtain closed-form (but in general suboptimal) solutions for transmit beamforming vector $\boldsymbol{v}$.

1) Direct-Channel SVD (D-SVD): The eigenvalue decomposition of $\boldsymbol{S}$ is represented by the precoding matrix $\boldsymbol{V}$ and the power allocation $\boldsymbol{\Sigma}$ in (2). In the D-SVD, the precoding matrix $\boldsymbol{V}$ is obtained from the SVD of $\boldsymbol{H}$, which can be expressed as $\boldsymbol{H} = \boldsymbol{Q}\boldsymbol{\Lambda}^{1/2}\boldsymbol{U}^{\dagger}$ where $\boldsymbol{Q} \in \mathbb{C}^{M_{r,s}\times M_s}$ and $\boldsymbol{U} \in \mathbb{C}^{M_{t,s}\times M_s}$ are matrices with othornormal columns, $M_s = \min(M_{t,s}, M_{r,s})$, and $\boldsymbol{\Lambda}$ is a $M_s \times M_s$ diagonal and positive matrix for which its diagonal elements are denoted by $\lambda_1 \geq \lambda_2 \geq \ldots \geq \lambda_{M_s}$. Let $\boldsymbol{V} = \boldsymbol{U}$, and furthermore, $\tilde{\boldsymbol{y}}(n) = \boldsymbol{Q}^{\dagger}\boldsymbol{y}(n)$ and $\boldsymbol{x}(n) = \boldsymbol{U}\tilde{\boldsymbol{x}}(n)$, the secondary user's MIMO channel in (1) can be equivalently written as

$$\tilde{\boldsymbol{y}}(n) = \boldsymbol{Q}^{\dagger}\boldsymbol{H}\boldsymbol{U}\tilde{\boldsymbol{x}}(n) + \tilde{\boldsymbol{z}}(n), \quad (20)$$

$$= \boldsymbol{\Lambda}^{1/2}\tilde{\boldsymbol{x}}(n) + \tilde{\boldsymbol{z}}(n), \quad (21)$$

where $\tilde{\boldsymbol{z}}(n) = \boldsymbol{Q}^\dagger \boldsymbol{z}(n)$ and $\tilde{\boldsymbol{z}}(n) \sim \mathcal{CN}(0, \boldsymbol{I})$. Notice that the D-SVD diagonalizes the MIMO channel and decomposes it into M_s parallel sub-channels with channel gains $\sqrt{\lambda_i}, i = 1, \ldots, M_s$.

Let $\boldsymbol{U} \triangleq [\boldsymbol{u}_1, \boldsymbol{u}_2, \ldots, \boldsymbol{u}_{M_s}]$, and $\alpha_i = ||\boldsymbol{g}\boldsymbol{u}_i||^2, i = 1, \ldots, M_s$. Considering the equivalent channel in (21) and noticing that $\mathbb{E}[\tilde{\boldsymbol{x}}(n)\tilde{\boldsymbol{x}}^\dagger(n)] = \boldsymbol{\Sigma}$, the optimal power assignments σ_i's can be obtained by solving the following equivalent problem (**P3**) derived from Problem **P2**:

$$\texttt{Maximize} \quad \sum_{i=1}^{M_s} \log_2 (1 + \lambda_i \sigma_i) \tag{22}$$

$$\texttt{Subject to} \quad \sum_{i=1}^{M_s} \sigma_i \leq P_t, \tag{23}$$

$$\sum_{i=1}^{M_s} \alpha_i \sigma_i \leq \gamma, \tag{24}$$

$$\sigma_i \geq 0, \forall i. \tag{25}$$

The optimal σ_i's for the above problem can be shown to have the following form of *multi-level* WF solutions:

$$\sigma_i = \left(\frac{1}{\nu + \alpha_i \mu} - \frac{1}{\lambda_i} \right)^+, \; i = 1, \ldots, M_s, \tag{26}$$

where ν and μ can be shown to be the non-negative Lagrange multipliers [23] associated with the transmit-power constraint in (23) and the interference-power constraint in (24), respectively, and can be obtained by the following algorithm (**A1**):

- **Given** $\mu \in [0, \hat{\mu}]$
- **Initialize** $\mu_{\min} = 0$, $\mu_{\max} = \hat{\mu}$
- **Repeat**
  1. Set $\mu \leftarrow \frac{1}{2}(\mu_{\min} + \mu_{\max})$.
  2. Find the minimum ν, $\nu \geq 0$, with which $\sum_{i=1}^{M_s} (\frac{1}{\nu + \alpha_i \mu} - \frac{1}{\lambda_i})^+ \leq P_t$. Substitute the obtained ν into (26) to obtain σ_i's.
  3. Update μ by the bisection method [23]: If $\sum_{i=1}^{M_s} \alpha_i \sigma_i \geq \gamma$, set $\mu_{\min} \leftarrow \mu$; otherwise, $\mu_{\max} \leftarrow \mu$.
- **Until** $\mu_{\max} - \mu_{\min} \leq \delta_\mu$ where δ_μ is a small positive constant that controls the algorithm accuracy.

Remark 3.1: If the interference-power constraint in (24) is inactive, it follows from the Karush-Kuhn-Tacker (KKT) conditions [23] that $\mu = 0$. From (26), the allocated powers can be then written as $\sigma_i = \left(\frac{1}{\nu} - \frac{1}{\lambda_i}\right)^+, \; i = 1, \ldots, M_s$, which become equal to the standard WF solutions with a constant water-level $\frac{1}{\nu}$. Hence, the D-SVD is indeed optimal if γ is sufficiently large such that the interference-power constraint is inactive.

Remark 3.2: If the secondary user's channel is MISO, it is not hard to verify that the D-SVD algorithm results in $\boldsymbol{S} = \boldsymbol{v}\boldsymbol{v}^\dagger$, where $\boldsymbol{v} = \frac{\sqrt{\min(\gamma, P_t)}}{||\boldsymbol{h}||}\boldsymbol{h}^\dagger$. Comparing it with the optimal $\boldsymbol{S}$ by Theorem 2, it follows that the D-SVD is optimal only if Case I of Theorem 2 is true, i.e., γ is sufficiently large such that the interference-power constraint is inactive.

2) Projected-Channel SVD (P-SVD): In the P-SVD, $\boldsymbol{S}$ is designed based on the so-called zero-forcing (ZF) criterion so as to completely avoid any interference at the primary receiver. It is noted that the ZF criterion has also been used in the MIMO broadcast channel (MIMO-BC) for design of downlink precoding that removes any co-channel interference between users (e.g., [28]-[29]). For the P-SVD, the secondary user's channel $\boldsymbol{H}$ is first projected into the null space of $\boldsymbol{g}^\dagger$ as

$$\boldsymbol{H}_\perp = \boldsymbol{H}\left(\boldsymbol{I} - \hat{\boldsymbol{g}}\hat{\boldsymbol{g}}^\dagger\right). \tag{27}$$

Let the SVD of the projected channel $\boldsymbol{H}_\perp$ be expressed as $\boldsymbol{H}_\perp = \boldsymbol{Q}_\perp\boldsymbol{\Lambda}_\perp(\boldsymbol{U}_\perp)^\dagger$. Then, the precoding matrix $\boldsymbol{V}$ for $\boldsymbol{S}$ is taken as $\boldsymbol{V} = \boldsymbol{U}_\perp$. From (27), by multiplying both the left-hand-side (LHS) and right-hand-side (RHS) with $\hat{\boldsymbol{g}}$, it can be verified that $(\boldsymbol{U}_\perp)^\dagger\hat{\boldsymbol{g}} = 0$. Since $\boldsymbol{S} = \boldsymbol{U}_\perp\boldsymbol{\Sigma}(\boldsymbol{U}_\perp)^\dagger$, it then follows that the resultant interference power at the primary receiver is zero, i.e., $\boldsymbol{g}\boldsymbol{S}\boldsymbol{g}^\dagger = 0$, and hence the interference-power constraint (12) for Problem **P2** is always satisfied for any γ, $\gamma \geq 0$.

Like the D-SVD, the P-SVD also diagonalizes the secondary user's MIMO channel. To see it, let $\bar{\boldsymbol{y}}(n) = (\boldsymbol{Q}_\perp)^\dagger\boldsymbol{y}(n)$ and $\boldsymbol{x}(n) = \boldsymbol{U}_\perp\bar{\boldsymbol{x}}(n)$, and the secondary channel in (1) can be equivalently represented by

$$\bar{\boldsymbol{y}}(n) = (\boldsymbol{Q}_\perp)^\dagger\boldsymbol{H}\boldsymbol{U}_\perp\bar{\boldsymbol{x}}(n) + \bar{\boldsymbol{z}}(n), \tag{28}$$

$$= (\boldsymbol{Q}_\perp)^\dagger(\boldsymbol{H}_\perp + \boldsymbol{H}\hat{\boldsymbol{g}}\hat{\boldsymbol{g}}^\dagger)\boldsymbol{U}_\perp\bar{\boldsymbol{x}}(n) + \bar{\boldsymbol{z}}(n), \tag{29}$$

$$= (\boldsymbol{Q}_\perp)^\dagger\boldsymbol{H}_\perp\boldsymbol{U}_\perp\bar{\boldsymbol{x}}(n) + \bar{\boldsymbol{z}}(n), \tag{30}$$

$$= (\boldsymbol{\Lambda}_\perp)^{1/2}\bar{\boldsymbol{x}}(n) + \bar{\boldsymbol{z}}(n), \tag{31}$$

where $\bar{\boldsymbol{z}}(n) = (\boldsymbol{Q}_\perp)^\dagger\boldsymbol{z}(n)$ and $\bar{\boldsymbol{z}}(n) \sim \mathcal{CN}(0, \boldsymbol{I})$, (29) is from (27), and (30) is by $\hat{\boldsymbol{g}}^\dagger\boldsymbol{U}_\perp = 0$. Because the projection in (27) reduces the channel rank at most by one, $\boldsymbol{\Lambda}_\perp$ has $M_s^\perp = \min(M_{t,s} - 1, M_{r,s})$ diagonal elements, denoted by $\lambda_1^\perp \geq \ldots \geq \lambda_{M_s^\perp}^\perp$. Hence, the secondary MIMO channel is decomposed into $M_s^\perp$ sub-channels with channel gains $\sqrt{\lambda_i^\perp}, i = 1, \ldots M_s^\perp$. The power allocation $\boldsymbol{\Sigma}$ for these sub-channels can be then obtained by considering the equivalent channel (31) with $\mathbb{E}[\bar{\boldsymbol{x}}(n)\bar{\boldsymbol{x}}^\dagger(n)] = \boldsymbol{\Sigma}$, as the standard WF solutions $\sigma_i = \left(\nu' - \frac{1}{\lambda_i^\perp}\right)^+$, $i = 1, \ldots, M_s^\perp$, where ν' is the constant water-level such that $\sum_{i=1}^{M_s^\perp} \sigma_i = P_t$.

Remark 3.3: If the interference-power constraint for Problem **P2** is indeed $\gamma = 0$, it is conjectured that the P-SVD is optimal. This conjecture is proved in Appendix IV.

Remark 3.4: If the secondary user's channel is MISO, it is not hard to verify that the P-SVD algorithm results in $\boldsymbol{S} = \boldsymbol{v}\boldsymbol{v}^{\dagger}$, where $\boldsymbol{v} = \sqrt{P_t}\frac{\beta_h}{||\beta_h||}\hat{\boldsymbol{h}}_{\perp}$. Comparing it with the optimal $\boldsymbol{S}$ by Theorem 2, it follows that the P-SVD is in general suboptimal unless $\gamma = 0$ and then Case II of Theorem 2 applies.

3) Performance Comparison: Comparing the computational complexity of the D-SVD and P-SVD, it is noticed that the former has a larger complexity for determining optimal power allocations due to the multi-level WF, while so does the latter for obtaining the precoding matrix due to the additional channel projection. In the following, the maximum achievable rate (or the capacity) for the secondary link by the optimal $\boldsymbol{S}$, and that by the two SVD-based algorithms are compared under two extreme scenarios: $P_t \to 0$ and $P_t \to \infty$, both under the assumption that γ is finite and $\gamma > 0$. Notice that the former case can also be considered as asymptotically low signal-to-noise ratio (SNR) at the secondary receiver (if the transmit power P takes its maximum value P_t) while the latter case as asymptotically high SNR.

As $P_t \to 0$, the D-SVD is the optimal solution. This can be easily verified similar like in Remark 3.1 by observing that the interference-power constraint in (12) eventually becomes inactive as $P_t \to 0$. In contrast, the P-SVD may incur a non-negligible rate loss in this case. This is so because the ZF-based projection causes part of the secondary user's channel energy to be lost. Since as $P_t \to 0$, both SVD-based algorithms assign the total transmit power to the sub-channel with the largest channel gain (λ_1 for the D-SVD and $\lambda_1^{\perp}$ for the P-SVD), it can be easily verified that the achievable rates of the D-SVD and P-SVD become $\log_2(1+\lambda_1 P_t)$ and $\log_2(1+\lambda_1^{\perp} P_t)$, respectively. Notice that $\lambda_1 \geq \lambda_1^{\perp}$. Because $\log(1+x) \cong x$ as $x \to 0$, the following theorem is obtained for the achievable rate by the optimal $\boldsymbol{S}$, the D-SVD and the P-SVD, denoted by R_{opt}, $R_{\text{D}-\text{SVD}}$, and $R_{\text{P}-\text{SVD}}$, respectively:

Theorem 3: As $P_t \to 0$, $R_{\text{opt}} = R_{\text{D}-\text{SVD}} = \frac{\lambda_1 P_t}{\log 2}$, and $R_{\text{P}-\text{SVD}} = \frac{\lambda_1^{\perp} P_t}{\log 2}$.

On the other hand, as $P_t \to \infty$, the achievable rate by the P-SVD becomes close to the secondary channel capacity achievable by the optimal $\boldsymbol{S}$. This is so because as P_t increases and eventually exceeds some certain threshold, any additional transmit power needs to be allocated into the projected channel $\boldsymbol{H}^{\perp}$ in order not to violate the interference-power constraint. From (31), it can be easily verified that as $P_t \to \infty$, the achievable rate of the P-SVD has a linear increase with $\log_2 P_t$ by a factor of $M_s^{\perp} = \min(M_{r,s}, M_{t,s} - 1)$, which is usually termed as the pre-log factor, the degree of freedom, or the spatial multiplexing gain in the literature. The following lemma states that R_{opt} also has a spatial multiplexing gain of $M_s^{\perp}$, indicating that the P-SVD is indeed optimal (in terms of the achievable spatial multiplexing gain) as $P_t \rightarrow \infty$.

Lemma 3: As $P_t \rightarrow \infty$, $\frac{R_{\text{opt}}}{\log_2 P_t} = \min(M_{r,s}, M_{t,s} - 1)$.

Proof: Please refer to Appendix V. ■

In contrast, the D-SVD may suffer a significant rate loss when $P_t \rightarrow \infty$. This can be observed from (24). Suppose $\alpha_i > 0, \forall i$, the total transmit power P is upper-bounded as $P = \sum_i \sigma_i \leq \frac{\gamma}{\min_i \alpha_i}$, regardless of the secondary user's own transmit power constraint P_t. As a result, the achievable rate of the D-SVD eventually gets saturated as $P_t \rightarrow \infty$, and the corresponding spatial multiplexing gain can be easily shown equal to zero. The above results are summarized in the following theorem:

Theorem 4: As $P_t \rightarrow \infty$, $\frac{R_{\text{opt}}}{\log_2 P_t} = \frac{R_{\text{P-SVD}}}{\log_2 P_t} = \min(M_{r,s}, M_{t,s} - 1)$, and $\frac{R_{\text{D-SVD}}}{\log_2 P_t} = 0$ if $\alpha_i > 0, i = 1, \ldots, M_s$.

IV. Multiple Primary Receivers

In this section, the general case of multiple primary receivers each having single or multiple receive antennas as shown in Fig. 1 is studied. Hence, Problem **P1** in (6)-(9) is considered.

A. MISO Secondary User's Channel

First, we consider the special case where the secondary user's channel is MISO. Like Lemma 1 in the case of one single-antenna primary receiver, it can be shown that the optimal transmit covariance matrix $\boldsymbol{S}$ in the case of multiple primary receivers/antennas still remains as a rank-one matrix when the secondary user's channel is MISO, i.e., beamforming is optimal. Hence, it follows that $\boldsymbol{S} = \boldsymbol{v}\boldsymbol{v}^{\dagger}$. However, a closed-form solution for the optimal beamforming vector $\boldsymbol{v}$ seems unlikely when the total number of antennas from all primary receivers $M_{r,p} = \sum_{k=1}^{M_k}$ is greater than one. Nevertheless, the optimal rank-one $\boldsymbol{S}$ for Problem **P1** can still be obtained using numerical optimization techniques like the interior-point method. Alternatively, the two SVD-based algorithms can also be modified to obtain suboptimal $\boldsymbol{v}$, as will be illustrated later in Section IV-B when the more general case of MIMO secondary user's channel is addressed.

In this subsection, we first consider Problem **P1** by substituting $\boldsymbol{S} = \boldsymbol{v}\boldsymbol{v}^{\dagger}$ into the problem. Then, based on this reformulated problem, we present alternative numerical optimization techniques that, in most cases, can be more efficient in terms of computational complexity than the interior-point method. The reformulated problem of Problem **P1** when the secondary user's channel is MISO, i.e., $\boldsymbol{H} \equiv \boldsymbol{h}$, can be expressed as (**P4**)

$$\texttt{Maximize} \quad \|\boldsymbol{h}\boldsymbol{v}\|^2 \tag{32}$$

$$\texttt{Subject to} \quad \|\boldsymbol{v}\|^2 \leq P_t, \tag{33}$$

$$\|\boldsymbol{G}_k\boldsymbol{v}\|^2 \leq \Gamma_k, \ k = 1, \ldots, K. \tag{34}$$

Notice that for the above problem although the two constraints specify a convex set for $\boldsymbol{v}$, the objective function is non-concave of $\boldsymbol{v}$ and hence renders Problem **P4** non-convex in its direct form. However, an interesting observation here is that if $\boldsymbol{v}$ satisfies the two constraints (33) and (34), so does $e^{j\theta}\boldsymbol{v}$ for any arbitrary θ, and the value of the objective function is maintained. Thus, without loss of generality we can assume that $\boldsymbol{h}\boldsymbol{v}$ is a real number. Using this assumption, Problem **P4** can be rewritten as

$$\texttt{Maximize} \quad \texttt{Re}(\boldsymbol{h}\boldsymbol{v}) \tag{35}$$

$$\texttt{Subject to} \quad \texttt{Im}(\boldsymbol{h}\boldsymbol{v}) = 0, \tag{36}$$

$$\|\boldsymbol{v}\|^2 \leq P_t, \tag{37}$$

$$\|\boldsymbol{G}_k\boldsymbol{v}\|^2 \leq \Gamma_k, \ k = 1, \ldots, K. \tag{38}$$

It can be shown that the above problem can be cast as a second-order cone programming (SOCP) [23], which can be solved by standard numerical optimization software.

Since Problem **P4** is indeed convex, and it can be further verified that the Slater's condition [23] that requires that the original (primal) problem needs to have a non-empty interior of the feasible set is satisfied for this problem, it follows that the strong duality holds for the problem at hand, which ensures that the duality gap between the original problem and its Lagrange dual problem is zero, i.e., solving the Lagrange dual problem is equivalent to solving the original problem. Motivated by this fact, as follows we will present an alternative solution for Problem **P4** by considering its Lagrange dual problem. First, the Lagrangian [23] of Problem **P4** can be expressed as

$$\mathcal{L}(\boldsymbol{v}, \nu, \{\mu_k\}) = \boldsymbol{v}^\dagger\boldsymbol{h}^\dagger\boldsymbol{h}\boldsymbol{v} - \nu\left(\boldsymbol{v}^\dagger\boldsymbol{v} - P_t\right) - \sum_{k=1}^{K}\mu_k\left(\boldsymbol{v}^\dagger\boldsymbol{G}_k^\dagger\boldsymbol{G}_k\boldsymbol{v} - \Gamma_k\right), \tag{39}$$

where ν and μ_k, $k = 1, \ldots, K$, are non-negative Lagrange multiplier (dual variable) associated with the transmit-power constraint in (33), and each interference-power constraint in (34), respectively. Let $\mathcal{D}_v$ be the set specified by the constraints (33) and (34), the Lagrange dual function [23] can be then defined as

$$f(\nu, \{\mu_k\}) = \max_{\boldsymbol{v} \in \mathcal{D}_v} \mathcal{L}(\boldsymbol{v}, \nu, \{\mu_k\}). \tag{40}$$

The Lagrangian dual problem [23] is then defined as

$$\min_{\nu \geq 0, \mu_k \geq 0, \forall k} f(\nu, \{\mu_k\}). \tag{41}$$

Notice that the Lagrangian in (39) can be rewritten as

$$\boldsymbol{v}^\dagger \left(\boldsymbol{h}^\dagger \boldsymbol{h} - \nu \boldsymbol{I} - \sum_{k=1}^{K} \mu_k \boldsymbol{G}_k^\dagger \boldsymbol{G}_k \right) \boldsymbol{v} + \nu P_t + \sum_{k=1}^{K} \mu_k \Gamma_k. \tag{42}$$

From the above expression, it follows that for solving the maximization problem so as to obtain the dual function in (40), the dual variables ν and $\{\mu_k\}$ must satisfy

$$\boldsymbol{h}^\dagger \boldsymbol{h} - \nu \boldsymbol{I} - \sum_{k=1}^{K} \mu_k \boldsymbol{G}_k^\dagger \boldsymbol{G}_k \preceq 0, \tag{43}$$

because otherwise, the optimal $\boldsymbol{v}$ that maximizes the Lagrangian in (42) will go unbounded to infinity, which contradicts the facts that the optimal value of the primal problem is bounded, and the duality gap is zero. Using (43), the dual problem in (41) can be expressed as (**P5**)

$$\texttt{Minimize} \quad \nu P_t + \sum_{k=1}^{K} \mu_k \Gamma_k \tag{44}$$

$$\texttt{Subject to} \quad -\boldsymbol{h}^\dagger \boldsymbol{h} + \nu \boldsymbol{I} + \sum_{k=1}^{K} \mu_k \boldsymbol{G}_k^\dagger \boldsymbol{G}_k \succeq 0, \tag{45}$$

$$\nu \geq 0, \tag{46}$$

$$\mu_k \geq 0, \; k = 1, \ldots, K. \tag{47}$$

The above problem can be efficiently solved using the standard semi-definite programming (SDP) software [23]. From the dual optimal solutions, the primal optimal solution for $\boldsymbol{v}$ can be obtained as any vector (may not be unique) that satisfies $\left(\boldsymbol{h}^\dagger \boldsymbol{h} - \nu \boldsymbol{I} - \sum_{k=1}^{K} \mu_k \boldsymbol{G}_k^\dagger \boldsymbol{G}_k \right) \boldsymbol{v} = 0$.

The computational complexity of three different methods for solving Problem **P1**, namely, the interior-point method, the SOCP for **P4**, and the SDP for **P5**, in the case of MISO secondary user's channel are compared as follows. All three methods have the similar order of complexity in terms of the number of (real) variables in each corresponding problem. For the interior-point method, the unknown $\boldsymbol{S}$ has $M_{t,s}$ real variables and $\frac{(M_{t,s}-1)M_{t,s}}{2}$ complex variables, results in a total number of real variables equal to $M_{t,s}^2$. The SOCP has the unknown $\boldsymbol{v}$ that has $2M_{t,s}$ real variables. The SDP has the unknown dual variables ν and $\{\mu_k\}$ that in total contribute to $K+1$ real variables. Consequently, the SOCP has a much lower computational complexity than the interior-point method. So does the SDP than the SOCP when, e.g., $K \ll M_{t,s}$. At last, it is noted that the SOCP and SDP have also been applied for design of downlink precoding for MIMO-BC channels (e.g., [31]-[32]).

B. MIMO Secondary User's Channel

When the secondary user's channel is MIMO, in general we have to resort to the interior-point method for solving Problem **P1**. Alternatively, the two SVD-based solutions developed in Section III in the case of one single-antenna primary receiver can also be modified to incorporate more than one primary receivers/antennas, as will be shown in this subsection.

1) Direct-Channel SVD (D-SVD): For the D-SVD, the precoding matrix $\boldsymbol{V}$ remains to be $\boldsymbol{U}$ obtained from the SVD of $\boldsymbol{H}$ regardless of the number of primary receivers or antennas. However, the power allocation $\boldsymbol{\Sigma}$ needs to be adjusted in order to incorporate multiple interference-power constraints in (3). By introducing a set of non-negative Lagrange multipliers, $\mu_1, \ldots, \mu_K$, each associated with one of K interference-power constraints in (3). Like Problem **P3** in the case of one single-antenna primary receiver, the optimal power assignments σ_i's in the case of multiple primary receivers/antennas can also be obtained as the *multi-level* WF solutions:

$$\sigma_i = \left(\frac{1}{\nu + \sum_{k=1}^{K} \sum_{j=1}^{M_k} \alpha_{i,k,j} \mu_k} - \frac{1}{\lambda_i} \right)^+, \ i = 1, \ldots, M_s, \tag{48}$$

where $\alpha_{i,k,j} = ||\boldsymbol{g}_{k,j} \boldsymbol{u}_i||^2$. Algorithm **A1** also needs to be modified so as to iteratively search for the optimal ν and μ_k's. Instead of updating a single μ by the bisection method in Algorithm **A1**, μ_k's can be simultaneously updated by the ellipsoid method [30] by observing that $\gamma_k - \sum_{i=1}^{M_s} \sum_{j=1}^{M_k} \alpha_{i,j,k} \sigma_i$ is a *sub-gradient* of $\mu_k, k = 1, \ldots, K$.

2) Projected-Channel SVD (P-SVD): Let $\boldsymbol{G} \in \mathbb{C}^{M_{r,p} \times M_{t,s}}$ denote the channel from the secondary transmitter to all primary receivers/antennas by taking each $\boldsymbol{g}_{k,j}$ as the $(\sum_{k'=1}^{k} M_{k'-1} + j)$-th row of $\boldsymbol{G}$, where $M_0 = 0$. Alternatively, $\boldsymbol{G} = [\boldsymbol{G}_1^T, \ldots, \boldsymbol{G}_K^T]^T$. Let the SVD of $\boldsymbol{G}$ be expressed as $\boldsymbol{G} = \boldsymbol{Q}_G \boldsymbol{\Lambda}_G^{1/2} \boldsymbol{U}_G^\dagger$. In order to avoid completely the interference at all primary receivers/antennas, the P-SVD obtains the precoding matrix $\boldsymbol{V}$ from the SVD of $\boldsymbol{H}_\perp$, which is the projection of $\boldsymbol{H}$ into the null space of $\boldsymbol{G}^\dagger$, i.e.,

$$\boldsymbol{H}_\perp = \boldsymbol{H}(\boldsymbol{I} - \boldsymbol{U}_G \boldsymbol{U}_G^\dagger). \tag{49}$$

Notice that the above matrix projection is non-trivial only when $M_{t,s} > M_{r,p}$, because otherwise a null matrix $\boldsymbol{H}_\perp$ is resulted. Let the SVD of $\boldsymbol{H}_\perp$ be expressed as $\boldsymbol{H}_\perp = \boldsymbol{Q}_\perp (\boldsymbol{\Lambda}_\perp)^{1/2} (\boldsymbol{U}_\perp)^\dagger$. Like the case of a single-antenna primary receiver, it can be verified that the secondary user's MIMO channel can be decomposed into $\min(M_{r,s}, M_{t,s} - M_{r,p})$ sub-channels with channel gains given by the diagonal elements of $\boldsymbol{\Lambda}_{\perp}$.

3) Hybrid D-SVD/P-SVD: A new hybrid D-SVD/P-SVD algorithm is proposed here in the case of multiple primary receivers/antennas, i.e., $M_{r,p} > 1$. In this algorithm, the secondary user's MIMO channel is first projected into the null space of some selected subspace of $\boldsymbol{G}^{\dagger}$ as opposed to the whole space spanned by $\boldsymbol{G}^{\dagger}$ in the P-SVD. Then, the D-SVD algorithm is applied to this projected channel to obtain transmit precoding matrix as well as power allocations that satisfy the interference-power constraints at the primary receivers. There are a couple of reasons for using this hybrid D-SVD/P-SVD algorithm. First, it works even if $M_{t,s} \leq M_{r,p}$ under which the P-SVD is not implementable. Secondly, in the case of a single-antenna primary receiver, i.e., $M_{r,p} = 1$, in Theorem 3 and Theorem 4, it has be shown that the D-SVD and P-SVD are asymptotically optimal as $P_t \to 0$ and $P_t \to \infty$, respectively. It is thus conjectured that when $M_{r,p} > 1$, the hybrid algorithm is likely to perform superior than both the D-SVD and P-SVD for some moderate values of P_t (as will be verified later by the simulation results in Section VI).

One important issue to address for the hybrid D-SVD/P-SVD algorithm is on the selection for the projected subspace of $\boldsymbol{G}^{\dagger}$. Although the optimal selection rule remains unknown, in this paper a heuristic rule is proposed as follows. First, each channel $\boldsymbol{g}_{k,j}$ in $\boldsymbol{G}$ is normalized by the corresponding $\sqrt{\Gamma_k}$ so as to make the equivalent interference-power constraints at all primary receivers equal to unity. Denote this normalized $\boldsymbol{G}$ as $\hat{\boldsymbol{G}}$. Next, let the SVD of $\hat{\boldsymbol{G}}$ be expressed as $\hat{\boldsymbol{G}} = \boldsymbol{Q}_{\hat{G}} \boldsymbol{\Lambda}_{\hat{G}}^{1/2} \boldsymbol{U}_{\hat{G}}^{\dagger}$, where the singular values in $\boldsymbol{\Lambda}_{\hat{G}}^{1/2}$ are ordered by $\lambda_{\hat{G},1} \geq \ldots \geq \lambda_{\hat{G},M_{\hat{G}}}$, $M_{\hat{G}} = \min(M_{t,s}, M_{r,p})$. The hybrid algorithm then projects $\boldsymbol{H}$ into the null space of the space spanned by the first b , $b \leq M_{\hat{G}}$, column vectors of $\boldsymbol{U}_{\hat{G}}$, denoted by $\boldsymbol{U}_{\hat{G}}(b)$, corresponding to the first b largest singular values of $\hat{\boldsymbol{G}}$, i.e.,

$$\boldsymbol{H}_{\perp}(b) = \boldsymbol{H}\left(\boldsymbol{I} - \boldsymbol{U}_{\hat{G}}(b)\left(\boldsymbol{U}_{\hat{G}}(b)\right)^{\dagger}\right). \tag{50}$$

After applying the precoding matrix $\boldsymbol{V}$ based on the SVD of $\boldsymbol{H}_{\perp}(b)$, it can be verified that the secondary user's MIMO channel is diagonalized and decomposed into $\min(M_{r,s}, M_{t,s} - b)$ sub-channels. Notice that if $b < M_{\hat{G}}$, there may be remaining interference at each primary receiver and, hence, the secondary transmitter power allocation $\boldsymbol{\Sigma}$ needs to be adjusted to make the interference-power constraints being satisfied at all primary receivers. This can be done by solving a similar problem like Problem **P3** in the D-SVD case.

The rational for the hybrid D-SVD/P-SVD algorithm lies in that only some selected subspace of $\hat{\boldsymbol{G}}^{\dagger}$ at the primary receivers is removed by the secondary transmit precoding, while the remaining subspace of $\hat{\boldsymbol{G}}^{\dagger}$ is preserved for the secondary transmission. Notice that the nulled subspace on the average contributes to the most amount of interference powers at the primary receivers because it corresponds to the first b largest singular values of $\hat{\boldsymbol{G}}$. For typical wireless channels, the channel from the secondary transmitter to each primary receive antenna (represented by the corresponding row vector of $\boldsymbol{G}$) is usually subject to variation or fading over time. Furthermore, these channels may exhibit quite different average channel gains (e.g., a near-far situation), and some of them may have certain correlations (e.g., for the receive antennas at the same primary receiver or for the primary receives located in the same vicinity). All these factors can result in a more spread distribution for the singular values in $\boldsymbol{\Lambda}_{\hat{G}}^{1/2}$, which thereby makes the subspace projection more effective in removing the interferences at the primary receivers. Because $\boldsymbol{G}$ is usually independent of the secondary MIMO channel $\boldsymbol{H}$, it is unlikely that the nulled subspace of $\hat{\boldsymbol{G}}^{\dagger}$ are strongly correlated with $\boldsymbol{H}$, a phenomenon termed *interference diversity*. Therefore, by selecting a proper value of b, the secondary user has a more flexibility in balancing between spacial multiplexing for the secondary transmission and interference avoidance at the primary receivers. Notice that the interference-diversity effect is in principle very similar to the *multiuser diversity* effect previously reported in the literature (e.g., [33]-[34]), which is exploited for multiuser rate scheduling in a mobile wireless network.

V. Multi-Channel Transmission

So far, we have considered the single-channel transmission for both primary and secondary users, and shown that even when some primary users are active for transmission, the secondary user is still able to achieve opportunistic spectrum sharing with active primary users by utilizing multiple transmit antennas and properly designing its transmit spatial spectrum. In this section, a more general multi-channel transmission is studied where both primary and secondary users transmit over parallel single-channels. This scenario is applicable when, e.g., both primary and secondary users transmit over multi-tone or orthogonal-frequency-division-multiplexing (OFDM) channels, or alternatively, over consecutive block-fading channels. For such scenarios, in order to achieve optimum spectrum sharing, the secondary user needs to first detect the primary user's transmission activities in all available dimensions of space, time and frequency and then adapts its transmit resources such as power, rate, and spatial spectrum at all of these dimensions. For convenience, in this section we consider the case of one single-antenna primary receiver in the CR network although the generalization to multiple primary receivers with single or multiple antennas can also be done similarly like in Section IV.

Let $\boldsymbol{H}_j$, $\boldsymbol{g}_j$ and $\boldsymbol{S}_j$ be defined the same as in Section III but now corresponding to one particular sub-channel $j, j = 1, \ldots, N$, where N is the total number of sub-channels for the multi-band transmission. Each sub-channel can be considered as, e.g., one OFDM tone in frequency domain or one fading block in time domain. It is assumed that the interference-power constraint γ is identical at all sub-channels. Problem **P2** can be then extended to the multi-channel transmission as (**P6**)

$$\texttt{Maximize} \quad \sum_{j=1}^{N} \log_2 \left| \boldsymbol{I} + \boldsymbol{H}_j \boldsymbol{S}_j \boldsymbol{H}_j^{\dagger} \right| \tag{51}$$

$$\texttt{Subject to} \quad \sum_{j=1}^{N} \texttt{Tr}(\boldsymbol{S}_j) \leq P_t, \tag{52}$$

$$\boldsymbol{g}_j \boldsymbol{S}_j \boldsymbol{g}_j^{\dagger} \leq \gamma, \forall j, \tag{53}$$

$$\boldsymbol{S}_j \succeq 0, \forall j. \tag{54}$$

This problem maximizes the total transmit rate over all of N sub-channels for the secondary transmission under a total transmit-power constraint and a set of interference-power constraints each for one of N sub-channels. Like Problem **P2**, the above problem can be shown to be convex and, hence, can be solved using standard convex optimization techniques. In the following, the *Lagrange dual-decomposition method* is applied to decompose Problem **P6** into N subproblems all having an identical structure. The main advantage of this method lies in that if the same computational routine can be simultaneously applied to all N subproblems, the overall computational time is maintained regardless of N. Other applications of the Lagrange dual-decomposition method for resource allocation in communication systems can be found in, e.g., [35]-[43].

For the problem at hand, the first step is to introduce the non-negative Lagrange multiplier ν associated with the power constraint in (52) and to write the Lagrangian of the original (primal) problem as

$$\mathcal{L}(\{\boldsymbol{S}_j\}, \nu) = \sum_{j=1}^{N} \log_2 \left| \boldsymbol{I} + \boldsymbol{H}_j \boldsymbol{S}_j \boldsymbol{H}_j^{\dagger} \right| - \nu \left(\sum_{j=1}^{N} \texttt{Tr}(\boldsymbol{S}_j) - P_t \right). \tag{55}$$

Let $\mathcal{D}_j$ be the set specified by the remaining constraints in (53) and (54) corresponding to sub-channel $j, j = 1, \ldots, N$. The Lagrange dual function is then defined as

$$f(\nu) = \max_{\boldsymbol{S}_j \in \mathcal{D}_j, \forall j} \mathcal{L}(\{\boldsymbol{S}_j\}, \nu). \tag{56}$$

The dual problem is then defined as $\min_{\nu \geq 0} f(\nu)$. It can be verified that the strong duality holds for the problem at hand, and hence the duality gap is zero. Therefore, the primal problem can be solved by first maximizing the

Lagrangian $\mathcal{L}$ to obtain the dual function $f(\nu)$, and then minimizing $f(\nu)$ over all non-negative values of ν.

Consider first the problem for obtaining $f(\nu)$ with some given ν. It is interesting to observe that $f(\nu)$ can be also written as

$$f(\nu) = \sum_{j=1}^{N} f'_j(\nu) + \nu P_t, \tag{57}$$

where

$$f'_j(\nu) = \max_{\boldsymbol{S}_j \in \mathcal{D}_j} \log_2 \left| \boldsymbol{I} + \boldsymbol{H}_j \boldsymbol{S}_j \boldsymbol{H}_j^\dagger \right| - \nu \mathtt{Tr}(\boldsymbol{S}_j), \; j = 1, \ldots, N. \tag{58}$$

Hence, $f(\nu)$ can be obtained by solving N independent subproblems, each for $f'_j(\nu)$, $j = 1, \ldots, N$. Each subproblem has the same structure and hence can be solved by using the same computational routine. This practice is usually referred to as the *dual decomposition*. From (58), each of these subproblems can be written more explicitly as (**P7**)

$$\mathtt{Maximize} \quad \log_2 \left| \boldsymbol{I} + \boldsymbol{H}_j \boldsymbol{S}_j \boldsymbol{H}_j^\dagger \right| - \nu \mathtt{Tr}(\boldsymbol{S}_j) \tag{59}$$

$$\mathtt{Subject\ to} \quad \boldsymbol{g}_j \boldsymbol{S}_j \boldsymbol{g}_j^\dagger \leq \gamma, \tag{60}$$

$$\boldsymbol{S}_j \succeq 0. \tag{61}$$

Compared with Problem **P2**, the above problem has the difference in that the transmit-power constraint in (11) is removed and a new term $\nu \mathtt{Tr}(\boldsymbol{S}_j)$ is subtracted in the objective function. This is a consequence of a total-power constraint over all N sub-channels in the multi-channel case instead of the per-sub-channel-based power constraint in the single-channel case. It can be verified that Problem **P7** is also convex and hence can be solved by using, e.g., the SOCP or SDP if the secondary user's channel is MISO (beamforming is optimal), or the interior-point method if the secondary user's channel is MIMO (spatial multiplexing is optimal).

The dual variable ν can be considered as a common price applied to all sub-channels for regulating their allocated transmit powers. It can be verified that in Problem **P7**, for each sub-channel, a larger ν will result in a smaller power consumption $\mathtt{Tr}(\boldsymbol{S}_j)$ and vice versa. Hence, the optimal ν can be found by a bisection search by comparing the optimal sum-power over all N sub-channels for a given ν with the transmit-power constraint P_t. In summary, the following algorithm (**A2**) can be used to solve Problem **P6**:

- **Given** $\nu \in [0, \hat{\nu}]$
- **Initialize** $\nu_{\min} = 0$, $\nu_{\max} = \hat{\nu}$

- **Repeat**
  1. Set $\nu \leftarrow \frac{1}{2}(\nu_{\min} + \nu_{\max})$.
  2. Solve Problem **P7** for $j = 1, \ldots, N$ independently to obtain $\{\boldsymbol{S}_j\}$.
  3. If $\sum_{j=1}^{N} \mathtt{Tr}(\boldsymbol{S}_j) \leq P_t$, set $\nu_{\max} \leftarrow \nu$; otherwise, $\nu_{\min} \leftarrow \nu$.
- **Until** $\nu_{\max} - \nu_{\min} \leq \delta_\nu$ where δ_ν is a small positive constant that controls the algorithm accuracy.

Algorithm **A2** can also be applied when the D-SVD or P-SVD algorithm is used to approximately solve each subproblem **P7**. The selection of the D-SVD or P-SVD at each sub-channel depends on the dual variable ν and the channels $\boldsymbol{H}_j$ and $\boldsymbol{g}_j$. Because $\boldsymbol{H}_j$ and $\boldsymbol{g}_j$ may change over different sub-channels, in order to exploit this diversity, the best selected SVD-based algorithm (the D-SVD or P-SVD) may also change from one sub-channel to another.

VI. Simulation Results

For the simulations, it is assumed that in the CR network both the channels from the secondary transmitter to the primary receivers $\boldsymbol{G}$, and to the secondary receiver $\boldsymbol{H}$, are drawn from the family of random vectors/matrices for which each element is generated by independent CSCG variable distributed as $\mathcal{CN}(0, 0.1)$ for $\boldsymbol{G}$, and $\mathcal{CN}(0, 1)$ for $\boldsymbol{H}$, respectively. The secondary user's transmit-power constraint P_t sweeps from 1 to 100, which is equivalent to a range of average SNRs per receive antenna (measured when the actual transmit power P is equal to P_t) from 0 dB to 20 dB. Monte Carlo simulations with 1000 randomly generated channel-pairs $(\boldsymbol{G}, \boldsymbol{H})$ are implemented, and the average achievable rates are plotted versus the SNR values. The results are shown for the following cases:

A. Capacity With (w/) versus Without (w/o) Interference-Power Constraint

Fig.2 compares the capacity for the secondary user's transmission w/ and w/o the interference-power constraint at a single-antenna primary receiver. In the case that the interference-power constraint is applied, γ is equal to 0.01. For the secondary receiver, it is assumed that $M_{r,s} = 1$, and two antenna configurations are considered for the secondary transmitter: (1) Single-input single-output (SISO) case: $M_{t,s} = 1$; (2) MISO case: $M_{t,s} = 4$. For both SISO and MISO secondary user's channels, it is observed that the interference-power constraint reduces the capacity of the secondary transmission, especially at the high-SNR regime. However, the capacity improvement by adding more transmit antennas at the secondary transmitter is observed to be substantial. This is so because in the SISO case, as SNR increases, the capacity is eventually limited by the interference-power constraint instead of the secondary user's own transmit power constraint; while in the MISO case, the secondary transmitter is able to apply transmit beamforming so as to avoid the interference at the primary receiver and at the same time, guarantee its own rate increase with SNR. Therefore, in addition to antenna array and diversity gains in the conventional MISO point-to-point transmission, multi-antennas at the secondary transmitter play another essential role in a CR network, i.e., adapting transmit spatial spectrum away from the interfering direction to the primary receiver, so as to achieve a high spectral efficiency for the secondary transmission.

B. D-SVD versus P-SVD

Fig. 3 shows the achievable rates of two SVD-based algorithms, the D-SVD and P-SVD, and compares them to the capacity w/ and w/o the interference-power constraint, as well as the achievable rate by a simple design for the secondary transmit spatial spectrum, termed *white spectrum*, for which equal power is allocated to all transmit antennas, i.e., $\boldsymbol{S} = \frac{P}{M_{t,s}}\boldsymbol{I}$. It is assumed that there is a single-antenna primary receiver, $\gamma = 0.1$, and $M_{t,s} = M_{r,s} = 2$. It is observed that the achievable rates by the D-SVD and P-SVD are close to the capacity w/ interference-power constraint at the low- and high-SNR regime, respectively. At the high-SNR regime, both the capacity by the optimal $\boldsymbol{S}$ obtained by numerical algorithm and the achievable rate by the P-SVD increase linearly with $\log_2 SNR$ by a factor of $\min(M_{r,s}, M_{t,s} - 1) = \min(2, 2-1) = 1$ while the achievable rate by the D-SVD eventually gets saturated, both in accordance with Theorem 4. Substantial rate improvements by the optimal as well as the D-SVD/P-SVD solutions over the simple white spectrum are also observed from low to high SNR values.

C. Hybrid D-SVD/P-SVD

Fig. 4 compares the achievable rates of the hybrid D-SVD/P-SVD with different values of b. The capacity w/ and w/o the interference-power constraint are also shown for comparison. It is assumed that the number of primary receivers $K = 2$ each with a single receive antenna, $\Gamma_k = 0.1, k = 1, 2$, and $M_{t,s} = M_{r,s} = 4$. Because there are two single-antenna primary receivers, the hybrid algorithm can choose to project the secondary user's channel $\boldsymbol{H}$ into either the whole space of $\hat{\boldsymbol{G}}^{\dagger}$ by taking $b = 2$ (or the P-SVD) or some selected subspace of $\hat{\boldsymbol{G}}^{\dagger}$ with $b = 1$, or simply choose not to project at all with $b = 0$ (or the D-SVD). It is observed that as SNR increases, the optimal SVD-based algorithm changes from the D-SVD to the hybrid D-SVD/P-SVD with $b = 1$, and finally to the P-SVD. This result is consistent with the conjecture we have made previously in Section IV-B.3. The rational here is that as the transmit power increases, the secondary user's transmit spatial spectrum also needs to allocate a larger portion of total transmit power into the projected channel in order not to violate the prescribed interference-power constraint at the primary receiver.

Fig. 5 compares the achievable rates of the hybrid D-SVD/P-SVD with the D-SVD and P-SVD as the number of single-antenna primary receivers K increases from 2 to 10. The interference-power constraint $\Gamma_k = 0.01$ is assumed to be equal at all primary receivers, and P_t is fixed as 10, and $M_{t,s} = M_{r,s} = 4$. Notice that for each given K, b for the hybrid algorithm can take values from 0 to $\min(M_{t,s}, K)$. If $b = 0$, the hybrid algorithm becomes the D-SVD; while if $b = \min(M_{t,s}, K)$, it becomes the P-SVD. In this figure, the achievable rate shown for the hybrid algorithm for each K is obtained by taking the maximum rate over all possible values of b. Notice that if $K \geq M_{t,s}$, the achievable rate by the P-SVD becomes zero because the ZF-based channel projection results in a null projected channel $\boldsymbol{H}_\perp$ in (49). It is observed that as K increases, the achievable rate by any of these three proposed algorithms decreases due to more added interference-power constraints. However, the hybrid algorithm by dynamically selecting b achieves substantial rate improvements compared with the D-SVD and P-SVD because it effectively exploits the interference-diversity gain in the CR network. As K becomes much larger than $M_{t,s}$, it is observed that the achievable rates by the hybrid algorithm and the D-SVD both converge to be identical. However, such convergence is observed to be very slow with respect to K.

D. Multi-Channel Transmission

A multi-tone or OFDM-based broadband transmission system is considered for a secondary user with $M_{t,s} = M_{r,s} = 2$ and a single-antenna primary receiver. The OFDM channels for both primary and secondary transmissions are assumed to have $N = 64$ tones, and four equal-energy, independent, and consecutive multi-path delays. The interference-power constraint at the primary receiver is set to be $\gamma = 0.1$ at all tones. In this case, the secondary user is able to allocate variable transmit rate, power, and spatial spectrum at different OFDM tones based on the channels $\boldsymbol{H}_j$ and $\boldsymbol{g}_j$, $j = 1, \ldots, N$. Fig. 6 shows the secondary user's capacity w/ and w/o the interference-power constraint, and the achievable rate of the per-tone-based suboptimal algorithm that selects the best SVD-based algorithm (the D-SVD or P-SVD) at each tone. It is observed that by exploiting the frequency-selective fading, the per-tone-based suboptimal algorithm achieves smaller gaps from the actual capacity w/ interference-power constraints compared with the case of single-channel transmission previously shown in Fig.3.

VII. Concluding Remarks and Future Directions

Transmit optimization for a single secondary MIMO/MISO link in a CR network under constraint of opportunistic spectrum sharing is considered. The capacity of the secondary link is studied under both the secondary transmit-power constraint and a set of interference-power constraints at multiple primary receivers. Multi-antennas are exploited at the secondary transmitter to optimally tradeoff between throughput maximization and interference avoidance. In the case of MISO secondary user's channel, beamforming is shown to be the optimal strategy for the secondary transmitter. In the case of MIMO secondary user's channel, the capacity-achieving transmit spatial spectrum under the interference-power constraint in general does not diagonalize the MIMO channel and hence requires sophisticated encoding and decoding methods. Two suboptimal algorithms based on the SVD of the secondary user's MIMO channel, namely the D-SVD and the P-SVD, are proposed to tradeoff between capacity and complexity. In the case of multiple primary receivers/antennas, a hybrid D-SVD/P-SVD algorithm is also proposed to exploit the inherent interference diversity gain in a CR network. The developed algorithms are also extended to the multi-channel transmission whereby the secondary user is able to employ transmit adaptations in all space, time and frequency domains so as to achieve optimum opportunistic spectrum sharing.

An interesting extension of this paper is to consider more generalized interference constraints at each primary receiver, especially when it is equipped with multiple receive antennas. Instead of considering either the per-antenna-based power constraint or the total-power constraint over all receive antennas, the interference constraint at each primary receiver can also be more specifically related to the primary user's channel capacity. More interestingly, both primary and secondary transmit adaptations can be jointly optimized under mutual interferences given their unequal priorities for spectrum utilization, through either a centralized control or distributed self-adaptations based on the principle of game theory. Results and algorithms developed in this paper can also be extended to the case where only statistical knowledge on the channel, instead of instantaneous channel knowledge as assumed in this paper, is available at the secondary transmitter for optimum design of transmit spatial spectrum under some long-term average interference-power constraints. Furthermore, although this paper addresses a single pair of secondary transmitter and receiver, it can also be extended to incorporate multiple secondary users that jointly share transmit spectrum with the primary users by considering different models of the secondary network, e.g., the uplink MIMO multiple-access channel (MAC), the downlink MIMO broadcast channel (BC), or the distributed MIMO interference channel (IC).

APPENDIX I
PROOF OF THEOREM 1

Consider the k-th primary transmission represented by

$$\boldsymbol{y}_k(n) = \boldsymbol{H}_k\boldsymbol{x}_k(n) + \boldsymbol{z}_k(n) + \boldsymbol{q}_k(n), \tag{62}$$

where $\boldsymbol{H}_k \in \mathbb{C}^{M_k\times N_k}$ denotes the k-th primary user's channel, M_k and N_k are the number of antennas at its receiver and transmitter, respectively; $\boldsymbol{y}_k(n)$ and $\boldsymbol{x}_k(n)$ are the received and transmitted signal vector, respectively; $\boldsymbol{q}_k(n)$ is the additive noise vector at the receiver that assumed to be distributed as $\boldsymbol{z}_k(n) \sim \mathcal{CN}(0, \phi_k\boldsymbol{I})$; $\boldsymbol{q}_k(n)$ is the interference from the secondary transmitter expressed as

$$\boldsymbol{q}_k(n) = \boldsymbol{G}_k\boldsymbol{x}(n). \tag{63}$$

It is easy to verify that the covariance matrix for $\boldsymbol{q}_k(n)$, denoted by $\boldsymbol{Q}_k = \mathbb{E}[\boldsymbol{q}_k(n)\boldsymbol{q}_k^\dagger(n)]$, is equal to $\boldsymbol{G}_k\boldsymbol{S}\boldsymbol{G}_k^\dagger$, where $\boldsymbol{S}$ is the transmit covariance matrix for the secondary user. Let the transmit covariance matrix of the k-th primary user be denoted by $\boldsymbol{S}_k$, $\boldsymbol{S}_k = \mathbb{E}[\boldsymbol{x}_k(n)\boldsymbol{x}_k^\dagger(n)]$. The capacity of the k-th primary transmission (in bits/complex dimension) can be then expressed as

$$C_1 = \log_2\left|\boldsymbol{I} + (\phi_k\boldsymbol{I} + \boldsymbol{Q}_k)^{-1/2}\,\boldsymbol{H}_k\boldsymbol{S}_k\boldsymbol{H}_k^\dagger\,(\phi_k\boldsymbol{I} + \boldsymbol{Q}_k)^{-1/2}\right|. \tag{64}$$

On the other hand, if the secondary transmitter if off, i.e., the interference from the secondary transmitter $\boldsymbol{q}_k(n)$ is nonexistent, the capacity of the k-th primary transmission is expressed as

$$C_2 = \log_2\left|\boldsymbol{I} + \frac{1}{\phi_k}\boldsymbol{H}_k\boldsymbol{S}_k\boldsymbol{H}_k^\dagger\right|. \tag{65}$$

The capacity loss of the k-th primary transmission due to the secondary transmission is then equal to $C_2 - C_1$. In order to find an upper-bound for such capacity loss, the following equalities/ineuqalities are provided for C_1:

$$\begin{aligned}
C_1 &= \log_2\left|\boldsymbol{I} + \boldsymbol{S}_k^{1/2}\boldsymbol{H}_k^\dagger\,(\phi_k\boldsymbol{I} + \boldsymbol{Q}_k)^{-1}\,\boldsymbol{H}_k\boldsymbol{S}_k^{1/2}\right|, && (66)\\
&\geq \log_2\left|\boldsymbol{I} + \frac{1}{\phi_k + \Gamma_k}\boldsymbol{S}_k^{1/2}\boldsymbol{H}_k^\dagger\boldsymbol{H}_k\boldsymbol{S}_k^{1/2}\right|, && (67)\\
&= \log_2\left|\boldsymbol{I} + \frac{1}{\phi_k + \Gamma_k}\boldsymbol{H}_k\boldsymbol{S}_k\boldsymbol{H}_k^\dagger\right|, && (68)\\
&\geq \log_2\left|\frac{\phi_k}{\phi_k + \Gamma_k}\left(\boldsymbol{I} + \frac{1}{\phi_k}\boldsymbol{H}_k\boldsymbol{S}_k\boldsymbol{H}_k^\dagger\right)\right|, && (69)\\
&= -\min(M_k, N_k)\log_2\left(1 + \frac{\Gamma_k}{\phi_k}\right) + C_2, && (70)
\end{aligned}$$

where (66) and (68) are due to $\log|\boldsymbol{I} + \boldsymbol{A}\boldsymbol{B}| = \log|\boldsymbol{I} + \boldsymbol{B}\boldsymbol{A}|$, (67) is from the facts that $\boldsymbol{Q}_k \preceq \Gamma_k\boldsymbol{I}$ and $\log|\boldsymbol{I} + \boldsymbol{A}\boldsymbol{X}_1\boldsymbol{A}^\dagger| \geq \log|\boldsymbol{I} + \boldsymbol{A}\boldsymbol{X}_2\boldsymbol{A}^\dagger|$, if $\boldsymbol{X}_1 \succeq \boldsymbol{X}_2 \succeq 0$. Using (70), the proof is completed.

APPENDIX II
PROOF OF LEMMA 1

Because Problem **P2** is convex, the optimal $\boldsymbol{S}$ must satisfy the Karush-Kuhn-Tacker (KKT) conditions [23] written at below:

$$\boldsymbol{h}^{\dagger}\left(1+\boldsymbol{h}\boldsymbol{S}\boldsymbol{h}^{\dagger}\right)^{-1}\boldsymbol{h}+\boldsymbol{\Phi} = \mu\boldsymbol{g}^{\dagger}\boldsymbol{g}+\nu\boldsymbol{I}, \tag{71}$$

$$\nu\left(\mathtt{Tr}(\boldsymbol{S})-P_t\right) = 0, \tag{72}$$

$$\mu\left(\boldsymbol{g}\boldsymbol{S}\boldsymbol{g}^{\dagger}-\gamma\right) = 0, \tag{73}$$

$$\mathtt{Tr}(\boldsymbol{\Phi}\boldsymbol{S}) = 0, \tag{74}$$

where ν, μ, and $\boldsymbol{\Phi}$ are the Lagrange multipliers associated with the constraint (11), (12) and (13), respectively, $\nu, \mu \geq 0, \boldsymbol{\Phi} \succeq 0$. First, consider the case of $\nu = 0$, from (72), it follows that $P < P_t$, i.e., P is not limited by the secondary transmit-power constraint, but instead, by the interference-power constraint. From (71) and because $\boldsymbol{\Phi} \succeq 0$, it follows that $\boldsymbol{g}$ must be in parallel to $\boldsymbol{h}$, i.e., $\boldsymbol{g} = c\boldsymbol{h}$, where c is a constant. In this case, it can be easily shown that the optimal $\boldsymbol{S}$ is $\boldsymbol{S} = \frac{\gamma}{||\boldsymbol{g}\boldsymbol{h}^{\dagger}||^2}\boldsymbol{h}^{\dagger}\boldsymbol{h}$, i.e., $\mathtt{Rank}(\boldsymbol{S}) = 1$. Next, consider the case of $\nu > 0$, i.e., $P = P_t$. In this case, the RHS of (71) has a full rank of $M_{t,s}$ regardless of μ. It then follows that at the LHS of (71), since the first term has a unit rank, $\mathtt{Rank}(\boldsymbol{\Phi}) \geq M_{t,s} - 1$. Since $\boldsymbol{S} \succeq 0$ and $\boldsymbol{\Phi} \succeq 0$, from (74) it follows that $\mathtt{Rank}(\boldsymbol{S}) + \mathtt{Rank}(\boldsymbol{\Phi}) \leq M_{t,s}$. Hence, $\mathtt{Rank}(\boldsymbol{S}) \leq 1$, and the proof is completed.

APPENDIX III
PROOF OF LEMMA 2

Let the optimal beamforming vector $\boldsymbol{v}' = \alpha_{v'}\hat{\boldsymbol{g}} + \beta_{v'}\hat{\boldsymbol{b}}$, where $\hat{\boldsymbol{b}}^{\dagger}\hat{\boldsymbol{g}} = 0$. It can be then verified that replacing $\hat{\boldsymbol{b}}$ with $\hat{\boldsymbol{h}}_{\perp}$ does not increase the interference power $||\boldsymbol{g}\boldsymbol{v}||^2$ in (16) since $(\hat{\boldsymbol{h}}_{\perp})^{\dagger}\hat{\boldsymbol{g}} = 0$, but always helps to improve the SNR at the secondary receiver $||\boldsymbol{h}\boldsymbol{v}||^2$ in (14) since $||\boldsymbol{h}\hat{\boldsymbol{h}}_{\perp}|| \geq ||\boldsymbol{h}\hat{\boldsymbol{b}}||$. The proof is then completed by the fact that the secondary user's capacity always increases with the receiver SNR.

APPENDIX IV
PROOF FOR OPTIMALITY OF P-SVD WHEN $\gamma = 0$

We show that if in the interference-power constraint (12) of Problem **P2**, $\gamma = 0$, the P-SVD is indeed optimal. First, using the constraint $\boldsymbol{g}\boldsymbol{S}\boldsymbol{g}^\dagger = \gamma = 0$, (10) can be simplified as

$$\begin{aligned} & \log_2 \left| \boldsymbol{I} + \boldsymbol{H}\boldsymbol{S}\boldsymbol{H}^\dagger \right| && (75)\\ = \ & \log_2 \left| \boldsymbol{I} + (\boldsymbol{H}_\perp + \boldsymbol{H}\hat{\boldsymbol{g}}\hat{\boldsymbol{g}}^\dagger)\boldsymbol{S}(\boldsymbol{H}_\perp + \boldsymbol{H}\hat{\boldsymbol{g}}\hat{\boldsymbol{g}}^\dagger)^\dagger \right|, && (76)\\ = \ & \log_2 \left| \boldsymbol{I} + \boldsymbol{H}_\perp\boldsymbol{S}(\boldsymbol{H}_\perp)^\dagger \right|, && (77) \end{aligned}$$

where (76) is from (27). Using (77), Problem **P2** with $\gamma = 0$ can be rewritten as

$$\begin{aligned} \texttt{Maximize} \quad & \log_2 \left| \boldsymbol{I} + \boldsymbol{H}_\perp\boldsymbol{S}(\boldsymbol{H}_\perp)^\dagger \right| && (78)\\ \texttt{Subject to} \quad & \texttt{Tr}(\boldsymbol{S}) \le P_t, && (79)\\ & \boldsymbol{g}\boldsymbol{S}\boldsymbol{g}^\dagger = 0, && (80)\\ & \boldsymbol{S} \succeq 0. && (81) \end{aligned}$$

Notice that without the constraint (80), the optimal $\boldsymbol{S}^*$ for the above problem should have the same form of $\boldsymbol{U}_\perp\boldsymbol{\Sigma}(\boldsymbol{U}_\perp)^\dagger$ as by the P-SVD. At last, it remains to check whether $\boldsymbol{g}\boldsymbol{S}^*\boldsymbol{g}^\dagger = 0$. This is so because $\hat{\boldsymbol{g}}^\dagger\boldsymbol{U}_\perp = 0$.

APPENDIX V
PROOF OF LEMMA 3

The following equalities/inequalities hold:

$$\begin{aligned} & \log_2 \left| \boldsymbol{I} + \boldsymbol{H}\boldsymbol{S}\boldsymbol{H}^\dagger \right| && (82)\\ = \ & \log_2 \left| \boldsymbol{I} + (\boldsymbol{H}_\perp + \boldsymbol{H}\hat{\boldsymbol{g}}\hat{\boldsymbol{g}}^\dagger)\boldsymbol{S}(\boldsymbol{H}_\perp + \boldsymbol{H}\hat{\boldsymbol{g}}\hat{\boldsymbol{g}}^\dagger)^\dagger \right|, && (83)\\ \le \ & \log_2 \left| \boldsymbol{I} + 2\boldsymbol{H}_\perp\boldsymbol{S}(\boldsymbol{H}_\perp)^\dagger + 2\boldsymbol{H}\hat{\boldsymbol{g}}\hat{\boldsymbol{g}}^\dagger\boldsymbol{S}(\boldsymbol{H}\hat{\boldsymbol{g}}\hat{\boldsymbol{g}})^\dagger \right| && (84)\\ \le \ & \log_2 \left| \boldsymbol{I} + 2\boldsymbol{H}_\perp\boldsymbol{S}(\boldsymbol{H}_\perp)^\dagger \right| + \log_2 \left| \boldsymbol{I} + 2\boldsymbol{H}\hat{\boldsymbol{g}}\hat{\boldsymbol{g}}^\dagger\boldsymbol{S}(\boldsymbol{H}\hat{\boldsymbol{g}}\hat{\boldsymbol{g}})^\dagger \right|, && (85) \end{aligned}$$

where (83) is from (27), (84) is by $(\boldsymbol{A}+\boldsymbol{B})\boldsymbol{S}(\boldsymbol{A}+\boldsymbol{B})^\dagger \preceq 2(\boldsymbol{A}\boldsymbol{S}\boldsymbol{A}^\dagger + \boldsymbol{B}\boldsymbol{S}\boldsymbol{B}^\dagger)$ for $\boldsymbol{S} \succeq 0$, (85) is by $\log|\boldsymbol{I} + \boldsymbol{S}_1 + \boldsymbol{S}_2| \le \log|\boldsymbol{I}+\boldsymbol{S}_1| + \log|\boldsymbol{I}+\boldsymbol{S}_2|$ for $\boldsymbol{S}_1, \boldsymbol{S}_2 \succeq 0$. Let $\mathcal{D}_S$ denote the set for $\boldsymbol{S}$ specified by (11), (12) and

(13), it then follows that

$$
\begin{aligned}
R_{\rm opt} &= \max_{\boldsymbol{S}\in\mathcal{D}_S} \log_2 \left|\boldsymbol{I}+\boldsymbol{H}\boldsymbol{S}\boldsymbol{H}^\dagger\right| && (86)\\
&\le \max_{\boldsymbol{S}\in\mathcal{D}_S} \log_2 \left|\boldsymbol{I}+2\boldsymbol{H}_\perp\boldsymbol{S}(\boldsymbol{H}_\perp)^\dagger\right| + \mathcal{O}(1), && (87)\\
&\le \max_{\boldsymbol{S}\in\mathcal{D}_S} \log_2 \left|2\left(\boldsymbol{I}+\boldsymbol{H}_\perp\boldsymbol{S}(\boldsymbol{H}_\perp)^\dagger\right)\right| + \mathcal{O}(1), && (88)\\
&\le R_{\rm P-SVD} + M_{r,s} + \mathcal{O}(1), && (89)
\end{aligned}
$$

where (87) follows from (85) by noticing that due to (12) the second term on the RHS of (85) is upper-bounded by some finite constant. From (89) and because $R_{\rm opt} \ge R_{\rm P-SVD}$, it follows that $\lim_{P_t\to\infty} \frac{R_{\rm opt}}{\log_2 P_t} = \lim_{P_t\to\infty} \frac{R_{\rm P-SVD}}{\log_2 P_t}$. Since it has already been verified in the main text that $\lim_{P_t\to\infty} \frac{R_{\rm P-SVD}}{\log_2 P_t} = \min(M_{r,s}, M_{t,s}-1)$, the proof is completed.

References

[1] Federal Communications Commission, "Facilitating opportunities for flexible, efficient, and reliable spectrum use employing cognitive radio technologies, notice of proposed rule making and order, FCC 03-322," Dec. 2003.

[2] J. Mitola and G. Q. Maguire, "Cognitive radios: making software radios more personal," *IEEE Personal Communications*, vol. 6, no. 4, pp. 13-18, Aug. 1999.

[3] S. Haykin, "Cognitive radio: brain-empowered wireless communications," *IEEE J. Sel. Areas Commun.*, vol. 23, no. 2, pp. 201-220, Feb. 2005.

[4] M. Gastpar, "On capacity under receive and spatial spectrum-sharing constraints," *IEEE Trans. Inf. Theory*, vol. 53, no. 2, pp. 471-487, Feb. 2007.

[5] A. Ghasemi and E. S. Sousa, "Fundamental limits of spectrum-sharing in fading environments," *IEEE Trans. Wireless Commun.*, vol. 6, no. 2, pp. 649-658, Feb. 2007.

[6] J. Huang, R. Berry, and M. L. Honig, "Auction-based spectrum sharing," *ACM/Springer Mobile Networks and Applications Journal (MONET)*, vol. 11, no. 3, pp. 405-418, Jun. 2006.

[7] Y. Xing, C. N. Mathur, M. A. Haleem, R. Chandramouli, and K. P. Subbalakshmi, "Dynamic spectrum access with QoS and interference temperature constraints," *IEEE Trans. Mobile Computing*, vol. 6, no. 4, pp. 423-433, Apr. 2007.

[8] H. Zheng and C. Peng, "Collaboration and fairness in opportunistic spectrum access," *Proc. IEEE Int. Conf. Comm. (ICC)*, vol. 5, pp. 3132-3136, May 2005.

[9] W. Wang and X. Liu, "List-coloring based channel allocation for open-spectrum wireless networks," *Proc. IEEE Veh. Technol. Conf. (VTC)*, pp. 690-694, Sep. 2005.

[10] S. A. Jafar and S. Srinivasa, "Capacity limits of cognitive radio with distributed and dynamic spectral activity," *IEEE J. Sel. Areas Commun.*, vol. 25, no. 3, pp. 529-537, Apr. 2007.

[11] N. Devroye, P. Mitran, and V. Tarokh, "Achievable rates in cognitive radio channels," *IEEE Trans. Inf. Theory*, vol. 52, no. 5, pp. 1813-1827, May 2006.

[12] A. Jovičić and P. Viswanath, "Cognitive radio: An information-theoretic perspective," *Proc. IEEE Int. Symp. Inf. Theory (ISIT)*, Jul. 2006.

[13] W. Wu, S. Vishwanath, and A. Arapostathis, "On the capacity of Gaussian weak interference channels with degraded message sets," *Proc. Conf. Inf. Sciences and Systems (CISS)*, Mar. 2006.

[14] I. Marić, A. Goldsmith, S. Shamai (Shitz), and G. Kramer, "On the capacity of interference channels with a partially-cognitive transmitter," *Proc. IEEE Int. Symp. Inf. Theory (ISIT)*, Jun. 2007.

[15] A. Jafar and Shlomo Shamai (Shitz), “Degrees of freedom of the MIMO X channel” , *Proc. IEEE Global Telecommun. Conf. GLOBECOM*, Dec. 2007.

[16] I. E. Telatar, “Capacity of multi-antenna Gaussian channels,” *Eur. Trans. Telecommun.*, vol. 10, no. 6, pp. 585-595, Nov. 1999.

[17] G. J. Foschini and M. J. Gans, “On limits of wireless communications in a fading environment when using multiple antennas,” *Wireless Personal Commun.*, vol. 6, no. 3, pp. 311-335, Mar. 1998.

[18] G. G. Raleigh and J. M. Cioffi, “Spatial-temporal coding for wireless communications,” *IEEE Trans. Commun.*, vol. 46, no. 3, pp. 357-366, Mar. 1998.

[19] V. Tarokh, N. Seshadri, and A. R. Calderbank, “Space-time codes for high data rate wireless communication: performance criterion and code construction,” *IEEE Trans. Inf. Theory*, vol. 44, no. 2, pp. 744-765, Mar. 1998.

[20] V. Tarokh, H. Jafarkhani, and A. R. Calderbank, “Space-time block codes from orthogonal designs,” *IEEE Trans. Inf. Theory*, vol. 45, no. 5, pp. 1456-1467, Jul. 1999.

[21] F. Rashid-Farrokhi, L. Tassiulas, and K. Liu, “Joint optimal power control and beamforming in wireless networks using antenna arrays,” *IEEE Trans. Commun.*, vol. 46, pp. 1313-1323, Oct. 1998.

[22] T. Cover and J. Thomas, *Elements of Information Theory,* New York: Wiley, 1991.

[23] S. Boyd and L. Vandenberghe, *Convex optimization,* Cambridge University Press, 2004.

[24] G. Caire and S. Shamai (Shitz), “On the capacity of some channels with channel state information,” *IEEE Trans. Inf. Theory*, vol. 45, no. 6, pp. 2007-2019, Sep. 1999.

[25] B. M. Hochwald and S. T. Brink, “Achieving near-capacity on a multiple-antenna channel,” *IEEE Trans. Commun.*, vol. 51, no. 3, pp. 389 - 399, Mar. 2003.

[26] J. M. Cioffi and G. D. Forney, “Generalized decision-feedback equalization for packet transmission with ISI and Gaussian noise,” in *Communications, Computation, Control and Signal Processing: a tribute to Thomas Kailath, A. Paulraj, V. Roychowdhury, and C. D. Shaper, Eds.*, 1997, Kluwer Academic Publishers.

[27] G. J. Foschini, “Layered space-time architecture for wireless communication,” *Bell Labs Technical Journal*, vol. 1, pp. 41-59, 1996.

[28] Q. H. Spencer, A. L. Swindlehurst, and M. Haardt, “Zero-forcing methods for downlink spatial multiplexing in multiuser MIMO channels”, *IEEE Trans. Signal Proc.*, vol. 52, no. 2, pp. 461-471, Feb. 2004.

[29] P. Tejera, W. Utschick, G. Bauch, and J. A. Nossek, “A novel decomposition technique for multiuser MIMO,” *Proc. Int. ITG Workshop on Smart Antennas*, Duisburg, Germany, Apr. 2005.

[30] R. G. Bland, D. Goldfarb, and M. J. Todd, “The ellipsoid method: A survey,” *Operations Research,* vol. 29, no. 6, pp. 1039-1091, 1981.

[31] M. Bengtsson and B. Ottersten, “Optimal downlink beamforming using semidefinite optimization”, *Proc. Allerton Conf. Comm. Control and Comp.*, pp. 987-996, Sep. 1999.

[32] A. Wiesel, Y. C. Eldar, and S. Shamai, “Linear precoding via conic optimization for fixed MIMO receivers”, *IEEE Trans. Sig. Proc.*, vol. 54, no. 1, pp. 161-176, Jan. 2006.

[33] R. Knopp and P.A. Humblet, “Information capacity and power control in single-cell multi-user communications,” *Proc. IEEE Conf. Comm. (ICC)*, pp. 331-335, 1995.

[34] P. Viswanath, D. Tse, and R. Laroia, “Opportunistic beamforming using dumb antennas,” *IEEE Trans. Inf. Theory,* vol. 48, no. 6, pp. 1277-1294, Jun. 2002.

[35] W. Yu, “A dual decomposition approach to the sum power Gaussian vector multiple access channel sum capacity problem,” *Proc. Conf. Inf. Sciences and Systems (CISS)*, Mar. 2003.

[36] L. Xiao, M. Johansson, and S. P. Boyd,“Simultaneous routing and resource allocation via dual decomposition,” *IEEE Trans. Commun.*, vol. 52, no. 7, pp. 1136-1144, Jul. 2004.

[37] R. Cendrillon, W. Yu, M. Moonen, J. Verlinden, and T. Bostoen, “Optimal multiuser spectrum balancing for digital subscriber lines,” *IEEE Trans. Commun.*, vol. 54, no. 5, pp. 922-933, May 2006.

[38] W. Yu and R. Lui “Dual methods for nonconvex spectrum optimization of multicarrier systems”, *IEEE Trans. Commun.*, vol. 54, no. 7, pp. 1310-1322, Jul. 2006.

[39] D. P. Palomar and M. Chiang, “A tutorial on decomposition methods for network utility maximization,” *IEEE J. Sel. Areas Commun.*, vol. 24, no. 8, pp. 1439-1451, Aug. 2006.

[40] M. Mohseni, R. Zhang, and John Cioffi, “Optimized transmission of fading multiple-access and broadcast channels with multiple antennas,” *IEEE J. Sel. Areas Commun.*, vol. 24, no. 8, pp. 1627-1639, Aug. 2006.

[41] R. Zhang, Y. C. Liang, R. Narasimhan, and J. M. Cioffi, “Approaching MIMO-OFDM capacity with per-antenna power and rate feedback,” *IEEE J. Sel. Areas Commun.*, vol. 25, no. 7, pp. 1284-1297, Sep. 2007.

[42] K. Seong, M. Mohseni, and J. Cioffi, “Optimal resource allocation for OFDMA downlink systems,” *Proc. IEEE Int. Symp. Inf. Theory (ISIT)*, Jul. 2006.

[43] C. Y. Chen, K. B. Seong, R. Zhang, and J. M. Cioffi, “Optimized transmission for upstream vectored DSL systems using zero-forcing generalized decision feedback equalizers,” *IEEE J. Sel. Topics Sig. Proc.*, Dec. 2007.

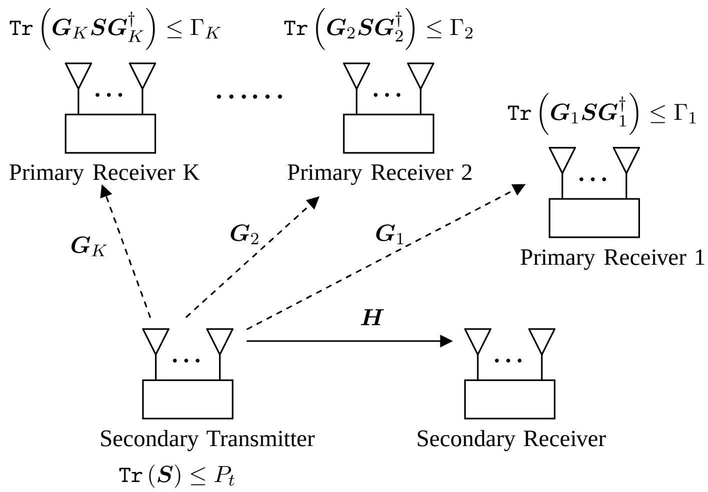

Fig. 1. A cognitive radio (CR) network where the secondary user shares the same transmit spectrum with K primary users.

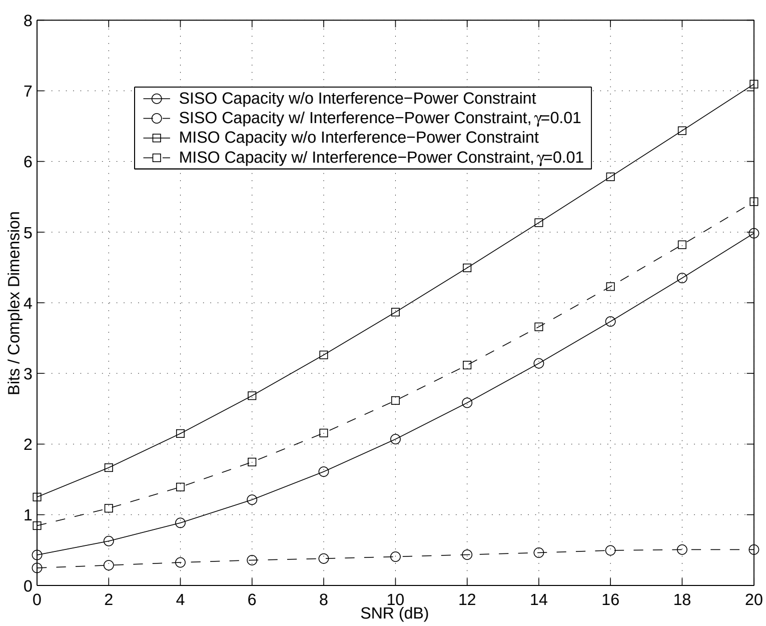

Fig. 2. Capacity comparison for the secondary transmission w/ and w/o the interference-power constraint at a single-antenna primary receiver.

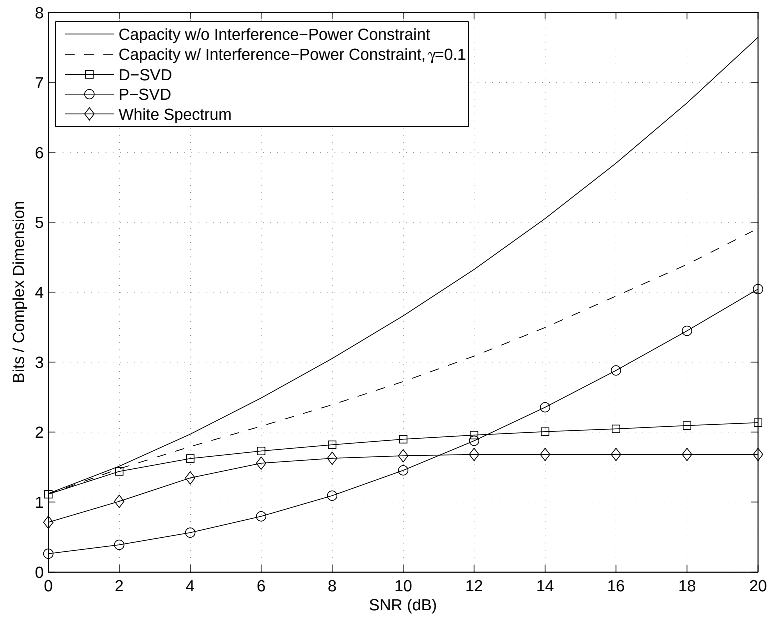

Fig. 3. Comparison of the achievable rates for the secondary transmission by the D-SVD and P-SVD in the case of a single-antenna primary receiver, and $M_{t,s} = M_{r,s} = 2$.

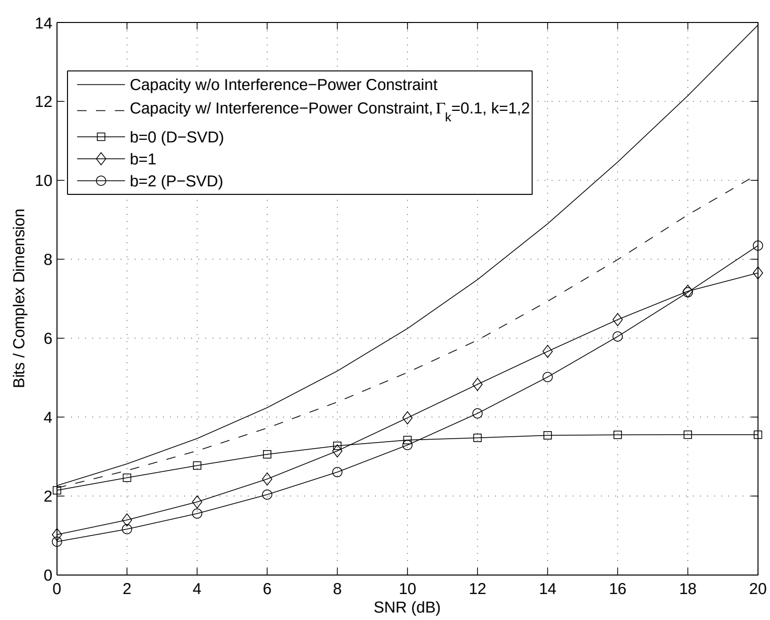

Fig. 4. Comparison of the achievable rates for the secondary transmission by the hybrid D-SVD/P-SVD with different values of b, in the case of two single-antenna primary receivers, and $M_{t,s} = M_{r,s} = 4$.

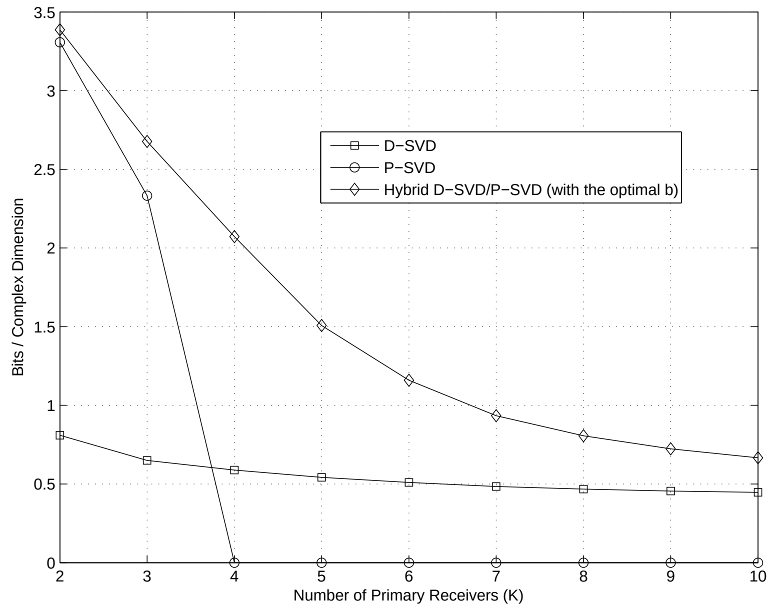

Fig. 5. Comparison of the achievable rates for the secondary transmission by the hybrid D-SVD/P-SVD, the D-SVD and the P-SVD for different number of single-antenna primary receivers K, in the case of $M_{t,s} = M_{r,s} = 4$ and a constant secondary power constraint $P_t = 10$.

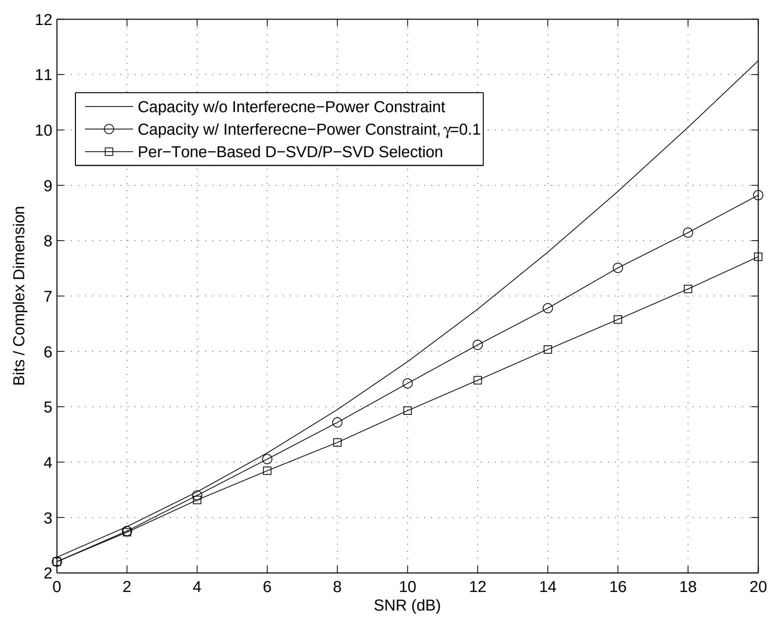

Fig. 6. Comparison of the achievable rates for the secondary transmission in a multi-tone-based broadband system with $N = 64$, a single-antenna primary receiver, and $M_{t,s} = M_{r,s} = 2$.